UNIVERSITÉ LIBRE DE BRUXELLES

Bruface
Brussels Faculty of Engineering

VRIJE UNIVERSITEIT BRUSSEL

Development of a Brain Computer Interface for robotic hand in the context of neuroscientific research about agency and body ownership

Gil Lauwers

Master thesis submitted under the supervision of
Prof. Dr. Ir. Bram Vanderborght
Prof. Dr. Ir. Dirk Lefeber

The co-supervision of
Ir. Albert De Beir
Dr. Emilie Caspar

In order to be awarded the Master's Degree in
Electro-mechanical Engineering,
Option Mechatronics-Construction

Academic year
2016-2017

Abstract

***'Development of a Brain Computer Interface for robotic hand in the context of neuroscientific research about agency and body ownership'*, Gil Lauwers, Electro-mechanical Engineering, Option Mechatronics-Construction, 2016-2017**

A Brain Computer Interface allows to use signals recorded from the brain to directly control an external device. This recent technology opens up new opportunities for numerous fields. In particular, a Brain Computer Interface controlling a robotic hand would help designing advanced paradigms to study the factors influencing the perception of autonomy of patients receiving a neuroprosthesis. Hence, the present work attempts to implement such a Brain Computer Interface for neuroscientific research. The input signal is the electroencephalographic activity recorded using a BioSemi ActiveTwo system. This signal is then processed using BCILAB, a Matlab toolbox. The Filter Bank Common Spatial Pattern algorithm was selected as feature extraction method. Feature vectors are classified using Linear Discriminant Analysis. The implemented BCI was tested in 3 steps. First, it was designed using publicly available data. Secondly, it was tested on a small sample of 6 participants. Finally, a pilot experiment was conducted in collaboration with Dr. Caspar from the Consciousness, Cognition & Computation Group from the Université Libre de Bruxelles. Obtained results were very promising and already allowed to validate 2 hypothesis that will be useful for the future neuroscientific experiments.

Keywords: Brain Computer Interface, Event-Related Desynchronization, Common Spatial Pattern, Linear Discriminant Analysis, BCILAB, Sense of agency

Acknowledgements

I would like to thank my promotors Prof. Dr. Ir. Bram Vanderborght and Prof. Dr. Ir. Dirk Lefeber without which I would not have had the opportunity to work on this very motivating topic.

I also thank Ir. Albert De Beir for his supervision. His valuable feedback helped me clarify my ideas and organize my work.

I would like to thank the Consciousness, Cognition & Computation Group for the help I received there and for the material they made available to me. More particularly, I want to thank Dr. Emilie Caspar for her help and her time. I appreciated working with her and I hope my work will help her in her research.

Finally, I want to thank my family and friends for their support, their corrections, and their time as participants for my experiments.

List of Abbreviations

BCI	Brain Computer Interface
Co3	Consciousness, Cognition & Computation Group
CSP	Common Spatial Pattern
EEG	Electroencephalographic
EMG	Electromyography
EOG	Electrooculography
ERD	Event-Related Desynchronization
ERS	Event-Related Synchronization
FBCSP	Filter Bank Common Spatial Pattern
FIR	Finite Impulse Response
fMRI	Functional Magnetic Resonance Imaging
HMM	Hidden Markov Model
IB	Intentional Binding
ICA	Independent Components Analysis
IIR	Infinite Impulse Response
LDA	Linear Discriminant Analysis
LSL	Lab Streaming Layer
MEG	Magnetoencephalographic
MLP	MultiLayer Perceptron
NN	Neural Networks
PCA	Principal Components Analysis
PET	Positron Emission Tomography
RMM	Robotics & MultiBody Mechanics Research Group
SpecCSP	Spectrally weighted Common Spatial Pattern
SVM	Support Vector Machine
TMS	Transcranian Magnetic Stimulation

Table 1: List of abbreviations

Contents

List of Figures

List of Tables

Chapter 1

Introduction

This chapter introduces the context in the field of Brain Computer Interface. First, the motivation behind the present work is detailed. Secondly, a short historical background is given.

1.1 Motivation

The goal of this thesis is to provide a Brain Computer Interface (BCI) to the Consciousness, Cognition & Computation Group (Co3) from the Université Libre de Bruxelles. One of the research topics of this research center is the study of free will, voluntary action and sense of agency (Caspar, Cleeremans, & Haggard, 2015; Caspar, Christensen, Cleeremans, & Haggard, 2016). The present work, promoted by the Robotics & MultiBody Mechanics Research Group (RMM) from the Vrije Universiteit van Brussel, mostly concerns the latter.

The sense of agency relates to the fact that we, as human, recognize that we are the authors of our voluntary actions, and of their consequences (Caspar et al., 2015). There are numerous studies on the various factors influencing this phenomenon. The context in which the Brain Computer Interface is implemented concerns the study of how agency is involved in the control of an external device.

A well-known paradigm in this research field is the Rubber Hand Illusion, in which the participant feels like a fake hand becomes his own (Botvinick, Cohen, et al., 1998). This feeling of body ownership happens when the same stimulation is applied to both the visible rubber hand and the hidden real hand of the subject. In a previous study, (Caspar et al., 2014) introduced a robotic hand controlled by a glove with sensors, which allowed to develop active paradigms for the Rubber Hand Illusion. The present work aims at designing and implementing a Brain Computer Interface in order to control the artificial hand directly with one's brain. This would allow to develop new paradigms and answer new questions

regarding the mechanisms involved in the sense of agency.

These mechanisms underlying the integration of an external object into one's body scheme are of high interest in the neuroscientific community but are also essential in the field of prosthesis. Indeed, having a better understanding of these phenomenon could help engineers design better adapted prosthesis and improve the quality of life of their users.

1.2 History

Brain Computer Interface is a rather new research field. The idea of using brain signals as an input command for communication and control is born with the discovery of the electroencephalographic (EEG) activity by Hans Berger in 1929 (Berger, 1929). However, very few researches were conducted on BCI's until the end of the 20th century. At that moment, the number of active BCI research groups grew from 6 in 1995 to more than 20 in 1999. This led to the organization of the first international meeting, which took place in 1999 and brought together 24 different research groups from United States, Canada, Great Britain, Germany, Austria, and Italy (Wolpaw et al., 2000). Since then, 5 other international meetings were held, with each time an increasing number of participants (see figure 1.1).

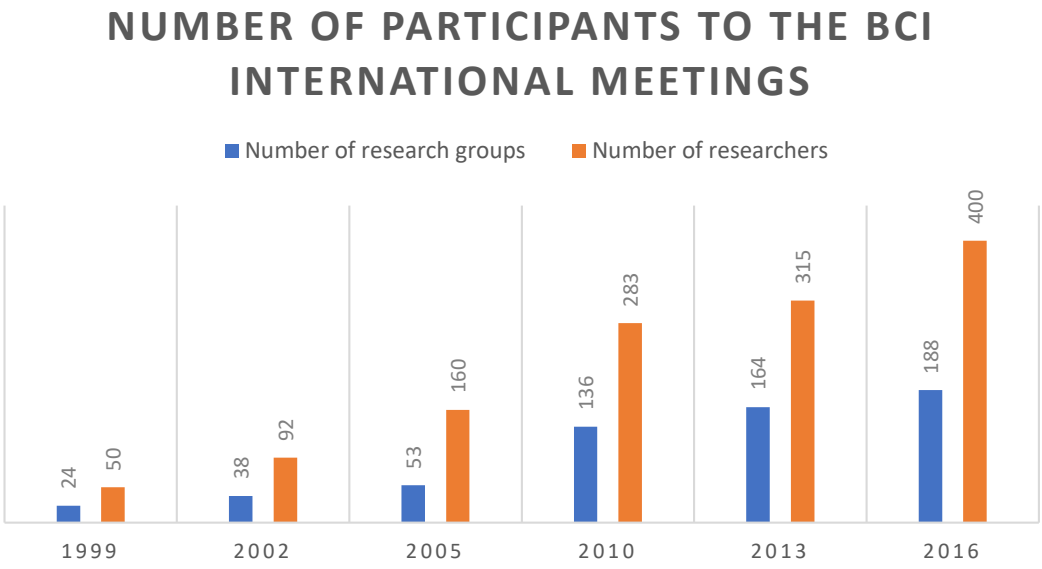

Figure 1.1: The number of participants has increased a lot since the first BCI International Meeting, as it can be seen from the data coming from the website of BCI society, which is organising these meetings.

In parallel with these meetings, 4 BCI competitions were organised in order

to compare the algorithms developed by the attending research groups. During these competitions, research labs provide data sets with the details about the acquisition procedure and an objective to reach. Results obtained by the participants can then be compared and provide interesting information about the efficiency of different methods.

Both these international meetings and competitions give a valuable overview of the evolution of the most important issues encountered in this recent but fast evolving field. Concerning the use of BCI's in the context of neuroscientific research, very few studies incorporate this new technology in their research about the sense of agency.

This chapter summarized first the motivation behind this master thesis (see section 1.1). The focus on the neurosciences is very important since it will dictate the design choices that will be made in chapter 3. The historical context given in section 1.2 described the BCI meetings and competitions that have been organized for almost 20 years. The meetings allow to see the evolution of most challenges in the field of BCI. Hence, it will be often referred to them in the State of the Art (see chapter 2). The data of the BCI competitions are publicly available. Hence, the BCI that will be implemented will be applied first on these data to compare its performance with the BCI's of the competititors (see chapter 4).

Chapter 2

State of the Art

This chapter summarizes the State of the Art in the field of Brain Computer Interface (BCI). First, the definition of a BCI is given and its general working principle is explained. After that, the different parts constituting a BCI are detailed. Finally, existing hardware and software tools are described.

2.1 Definition and working principle

A definition of a Brain Computer Interface was given in (Wolpaw et al., 2000):"*A brain-computer interface is a communication system that does not depend on the brain's normal output pathways of peripheral nerves and muscles*". Consequently, electrical potentials arising from eye movements or jaw clenching are considered as artifacts and must be avoided. The general working principle was defined as follows: "*Like any communication and control system, a BCI has an input, an output, and a translation algorithm that converts the former to the latter*".

In more recent work, the working principle of BCI's is more often divided as follows (see figure 2.1):

1. Acquisition
2. Preprocessing or processing
3. Feature extraction
4. Translation or classification
5. Output and feedback

The input as defined in the citation from (Wolpaw et al., 2000) groups together the acquisition, the processing and the feature extraction. The translation

between input and output is performed through the classifier. In real application, the output of the BCI often serves as a feedback. In neuroscientific research, various types of visual or auditory feedback are used.

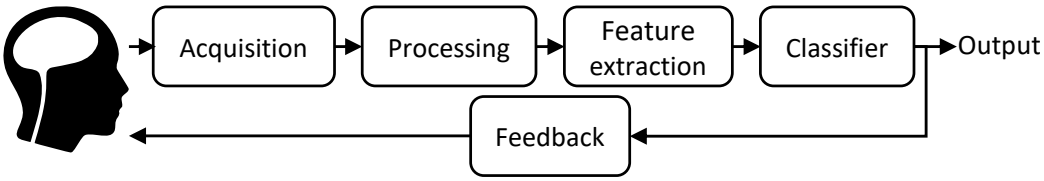

Figure 2.1: The acquisition consists in acquiring continuous signals from the brain and digitizing them. Those signals are then filtered both temporally and spatially during the processing phase. Artifacts are also removed during this step. After that, particular features of the signals are extracted in order to provide an input vector to the classifier. The output depends on the application and can be returned to the user under various form of feedback.

2.2 Building a Brain Computer Interface

2.2.1 Acquisition

The acquisition is the first building block of a Brain Computer Interface. The brain state and activity is reflected in a wide variety of measurable signals. These potential input signals are reviewed in the part of this section. As it will be demonstrated, the electroencephalography (EEG) is the most adapted method for this thesis. Consequently, the second part of this section is focused on this category of signal only and details two different types of electrodes that can be used to record it.

Potential input signals

The brain signals that are the most commonly used are the electrical currents that result from the firing of neurons. These electrical signals can be measured directly or indirectly. The direct or invasive method consists of electrodes measuring individual cortical neurons, therefore implanted in the brain. The indirect or noninvasive method consist of scalp electrodes measuring the electroencephalographic (EEG) activity . Although, the first BCI's were using both invasive or noninvasive method (Wolpaw et al., 2000), the surgery needed for invasive methods makes them clearly unsuitable for this thesis.

Among the noninvasive methods, some are based on nonelectrical signals. Magnetic fields can be recorded using magnetoencephalographic (MEG) activity. Changes in blood pressure and in metabolism can be measured through

functional magnetic resonance imaging (fMRI), positron emission tomography (PET) or infrared imaging. However, the costs and physical dimensions of these acquisition methods are prohibitive and clearly make them unsuitable for the present work (Vaughan et al., 2003). Moreover, metabolic changes involve long time-constants, which is a non negligible drawback for real time BCI's (Cincotti et al., 2006).

Consequently, most BCI's are based on EEG and so is the one developed in this thesis.

Wet versus dry electrodes

Most EEG recording devices are using wet electrodes requiring the application of an electrolyte gel under each electrode in order to increase electrical conduction, what leads to a non negligible preparation time and can be inconvenient for the subject under test, which has to be patient before the recording and has to wash his hair after to remove the sticky gel. The use of dry electrodes can considerably reduce the setup time and improve the trial conditions for the subject (Vaughan & Wolpaw, 2011). In (Grozea, Voinescu, & Fazli, 2011), the use of self developed dry electrodes gave results similar to the classic gel-based electrodes. However, as stated in (Lopez-Gordo, Sanchez-Morillo, & Valle, 2014), which reviewed a wide variety of dry electrodes, there is a need for homogenization of the methods used for characterization and evaluation of performance of the different types of electrodes to be able to conveniently compare them and draw conclusion about their efficiency.

2.2.2 Processing

The second building block of a Brain Computer Interface is the processing. The goal of this processing step is to maximize the signal-to-noise ratio (Wolpaw et al., 2000). It is then essential to first describe the signal and the possible sources of noise. This is done in the first part of this section. After that, various types of filtering methods aiming at enhancing the former with respect to the latter are detailed.

Signal and sources of noise

Signal A typical EEG signal, measured from the scalp, has an amplitude of about $10\mu V$ to $100\mu V$ and a frequency in the range of $1Hz$ to about $100Hz$ (Subha, Joseph, Acharya, & Lim, 2010). In general, the EEG frequencies that are studied are below 50Hz. This spectrum is divided in several frequency bands that are related to certain mental states and brain activities. The limits between

these frequency bands vary from one paper to the other. In (Buzsaki, 2006), they are defined as follows:

- δ band: $0.5 - 4Hz$
- θ band: $4 - 8Hz$
- α band: $8 - 12Hz$
- β band: $12 - 30Hz$
- γ band: $> 30Hz$

Next to this temporal division, the spatial distribution also plays a fundamental role. The areas of the brain involved in the process of moving one's hand are the motor cortex and the somatosensory cortex (see figure 2.2a). In the 10-20 system used for the placement of the electrodes, these areas correspond to electrodes C3, Cz and C4 (see figure 2.2b).

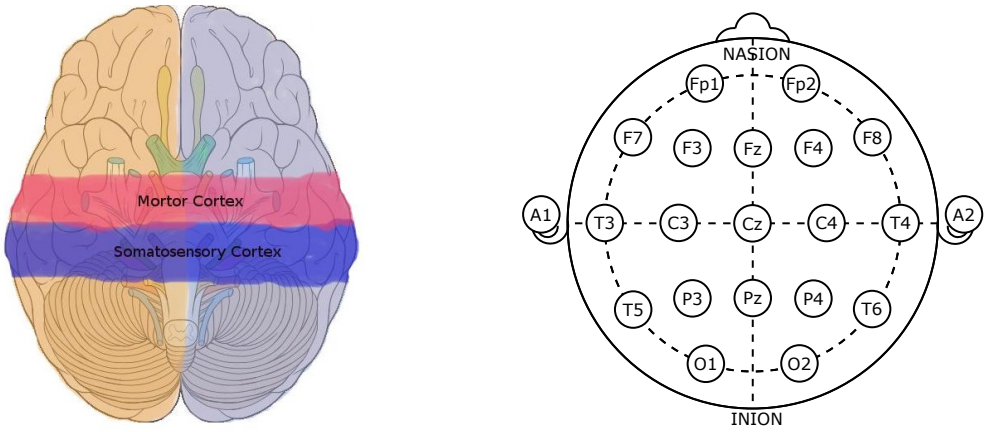

(a) Areas of the brain involved in the process of moving one's hand.

(b) 10-20 system used for the placement of the electrodes.

Figure 2.2: The area of the brain involved in the process of moving one's hand are the motor cortex and the somatosensory cortex. The EEG activity of these areas is measured by electrodes C3, Cz and C4.

When located at these motor area, the α band is called Rolandic α, central α, somatosensory α, or more frequently: the μ band. This μ rhythm is a motor-relaxation-associated rhythm whose amplitude is directly impacted by voluntary movement (Buzsaki, 2006). These changes in the amplitude of a particular frequency band are called Event-Related Desynchronization and Synchronization (ERD/ERS). ERD/ERS are decreases or increases of power in given frequency

bands, resulting from a decrease or an increase of the synchrony of the underlying neurons (Pfurtscheller & Da Silva, 1999).

ERD/ERS can be observed in several frequency bands and reflect the activity in the concerned frequency band. The μ band being a motor-associated rhythm, Event-Related Desynchronization and Synchronization in this band reflect the motor activity. It has been shown that ERD in the μ band are observed not only when movements occur but also when movement are imagined or are observed (see figure 2.3). Neurons involved in this process are called mirror neurons (Pineda, Allison, & Vankov, 2000).

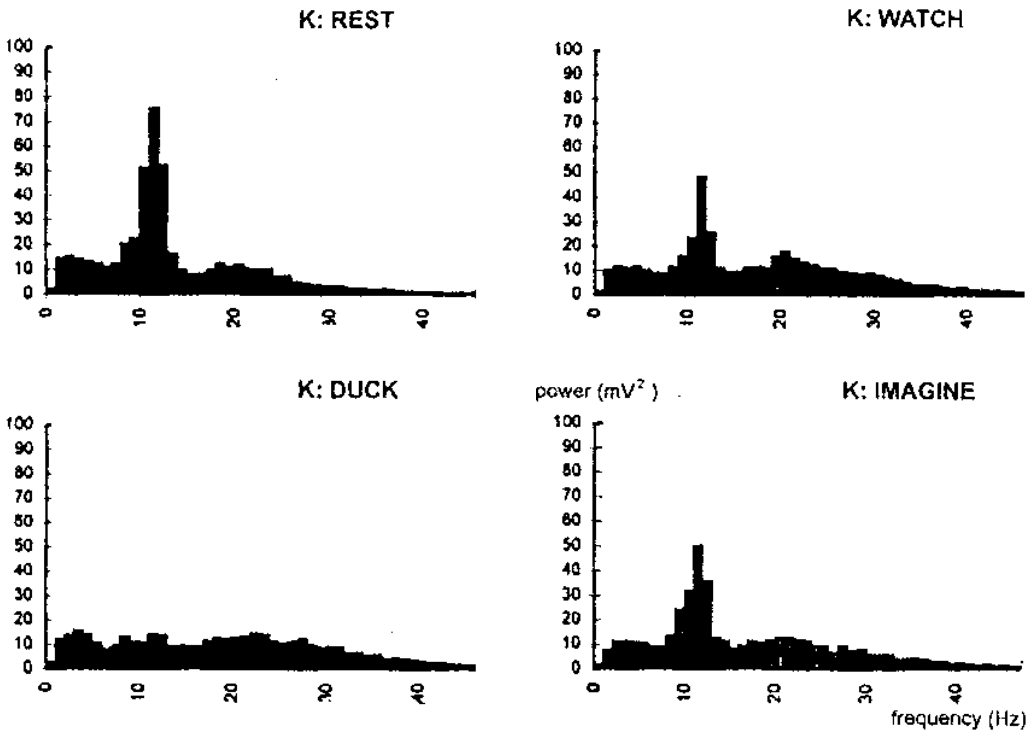

Figure 2.3: The power are obtained for $120s$ of recordings for each of the four classes. The decrease of power in the μ band $(8-12Hz)$ resulting from the Event-Related Desynchronization (ERD) is observable when the movements occur, are observed or are imagined. The difference between these 3 classes are reflected in the amplitude of the decrease of power (Pineda et al., 2000).

Sources of noise Noise in BCI applications can have both neuronal and non-neuronal sources. Indeed, any brain feature different from the one that is chosen as control signal is considered as noise and must thus be minimized. Nonneuronal sources of noise can be nonphysiological, such as the $50Hz$ from the grid, or physiological, such as electrical signals caused by muscular activity. Nonneuronal

sources of noise are often called artifacts. Similarly to neuronal source of noise, they can not interfere with the signal controlling the Brain Computer Interface. The most important sources of artifacts are the eye movements and the muscular activity (Fatourechi, Bashashati, Ward, & Birch, 2007).

Eye artifacts, measured by electrooculography (EOG), have a high amplitude and a frequency content mostly below $4Hz$. They are maximum over the anterior head regions. Figures 2.4a and 2.4b show examples of data recorded with and without eye artifacts. Figures 2.4c and 2.4d show the frequency content associated to these two conditions. The data used for these figures come from the data set IIa of the BCI competition IV (Tangermann et al., 2012).

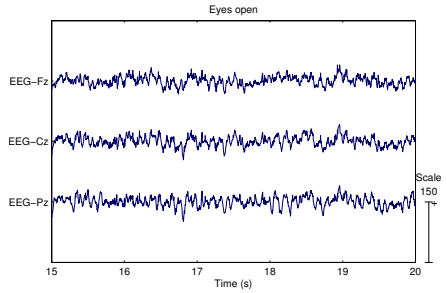

(a) EEG signal recorded eyes open.

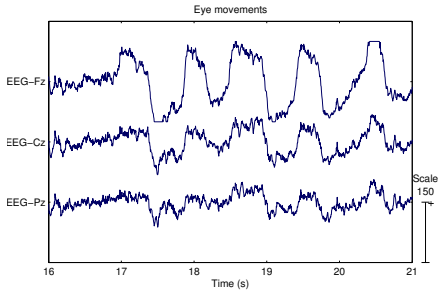

(b) EEG signal recorded during eye movements.

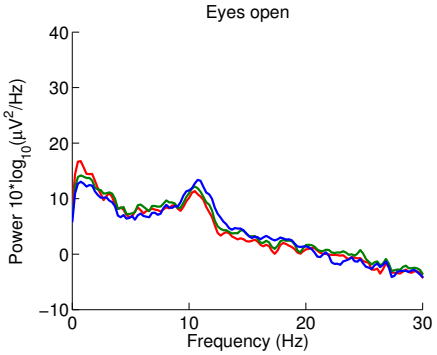

(c) Spectrum of EEG recorded eyes open at electrodes.

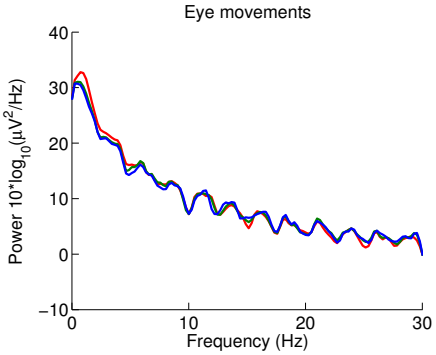

(d) Spectrum of EEG recorded during eye movements.

Figure 2.4: These signals are recorded from electrodes Fz, Cz and Pz. The electrode Cz is central, electrode Fz is positioned more upfront while electrode Pz is more backfront (see figure 2.2b for the exact position). Slow signals of high amplitudes are observable during eye movements. The amplitude of these signals is bigger at the most frontal electrode Fz. The power in the low frequencies is considerably increased in presence of eye artifacts.

Muscular artifacts, measured by electromyography (EMG), have also a high amplitude. However, they are maximum at higher frequencies, typically above

$30Hz$. Typical muscular artifacts were extracted from the data of data set IIa of the BCI competition IV and are shown in figure 2.5.

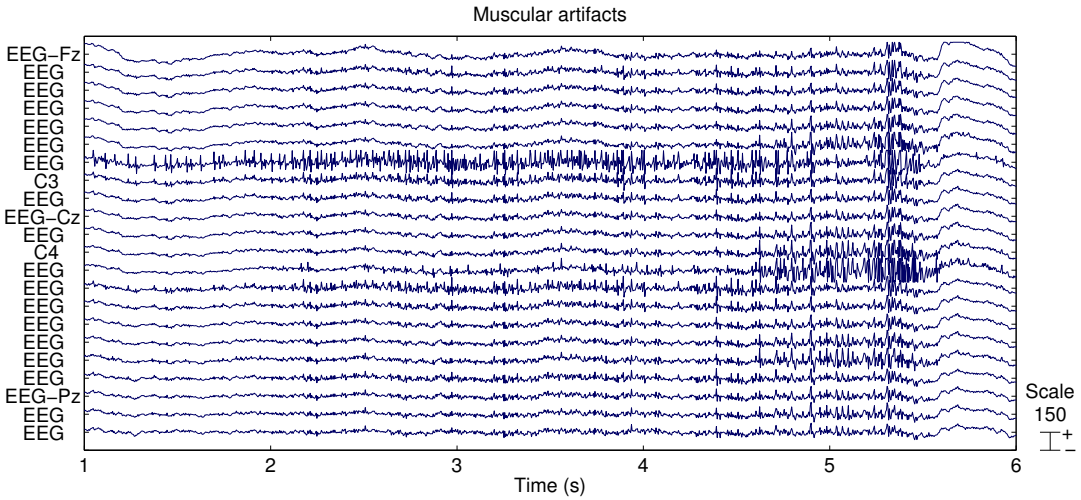

Figure 2.5: Muscular artifacts are reflected in high frequency signals of high amplitude.

Next to these physiological artifacts, non-physiological artifacts must also be dealt with. These are most of the time easier to eliminate as their frequency range is more limited. For example, the 50Hz line noise can be filtered out using a notch filter or using a battery supplied acquisition device.

Processing method

As explained before, the processing step aims at improving the signal-to-noise ratio. Now that the signal and the sources of noise have been described, adapted methods must be implemented to reduce the noise without altering the signal. First, different methods of handling artifacts will be presented. Second, classical signal processing tools such as rereferencing, resampling and filtering will be reviewed.

Artifacts There are different ways of handling artifacts. In (Fatourechi et al., 2007), these are grouped in the 3 following classes:

1. **Artifact avoidance**(Fatourechi et al., 2007): Artifact avoidance consists in asking the participants to avoid eye movements and muscle contractions. This method is the easiest to implement as it only requires the experimenter to give proper instructions to the participants. However, it is most often only possible to limit artifacts to some extend and not completely avoid them as many are involuntary.

2. **Artifact rejection**(Fatourechi et al., 2007): Artifact rejection consists in rejecting the trials in which artifacts have occurred. For offline analysis of the data, the affected trials can be identified by visual inspection. This requires human labor but allows to avoid additional computational resources. However, as soon as the Brain Computer Interface is tested online, automatic rejection methods have to be used because manual rejection cannot be performed in real time. Automatic rejection can be implemented by discarding the signal whenever a particular characteristics of the signal exceeds a certain threshold. Artifact rejection is not very computationally demanding but has the disadvantage to lead to a loss of a non negligible portion of the signal. For real-time application, this means that the system is not controllable during these periods.

3. **Artifact removal** (Fatourechi et al., 2007): Artifact removal consists in removing the artifacts from the signal without altering its neurological content. Artifact removal methods are more computationally demanding but allow to control the BCI without interruption. When the frequency range of the artifacts do not overlap the frequency range of the useful signal, linear filtering is the easiest and most suitable method. For BCI driven by the desynchronization of the μ and β bands (ranging approximately from $8Hz$ to $30Hz$), the low frequency eye artifacts can be highpass filtered while the high frequency EMG artifacts can be lowpass filtered. This method can not be used with BCI's based on the slow potentials since their frequency content is superimposed to the one of the eye artifacts.

   Linear combination and regression allows to solve this problem. This method requires the use of external electrodes. It is therefore most suitable for eye artifacts where EOG electrodes can be placed around the eyes then for EMG artifacts that can come from any facial muscles. The principle of linear combination and regression is to remove a fraction of the EOG signal from the contaminated EEG signal to obtained an EEG signal free from eyes artifacts. One limitation of that method is that the EOG electrodes are also contaminated with the EEG signal so that a part of the signal is lost when the EOG signal is subtracted.

   Finally, statistical methods such as Independent Components Analysis (ICA) or Principal Components Analysis (PCA) try to mathematically decompose the signal into a set of components, some of them being related to physical phenomena. These methods do not require any additionnal external electrodes but often require visual inspection to identify the components related to artifacts. Similar to the previous method, ICA and PCA have mostly been used for identifying eye artifacts rather than muscular artifacts.

A complete review of the literature concerning artifacts in BCI systems can be found in (Fatourechi et al., 2007). In their review, they observed that:

1. many papers do not report about handling artifacts
2. manual rejection is the most used method
3. only few studies perform automatic rejection or removal of artifacts.

In the last BCI competition (Tangermann et al., 2012), datasets IIa and IIb were dealing with motor imagery contaminated with eye artifacts. Three EOG electrodes were provided in both datasets. For both datasets, the winning algorithm used linear filtering to handle the artifacts.

Signal processing tools This section reviews the principal methods used in signal processing in the BCI field.

- **Rerefencing**:
  EEG acquisition devices record the signals with respect to a given reference. (Hagemann, Naumann, & Thayer, 2001) stated that the use of different referencing methods impacts the results of the study. The quality of a measured signal is function of the activity of the electrode of interest and of the reference. The electrical signal at the electrode of interest is the signal while the activity at the reference electrode is the noise. There are three main referencing methods (Al-ani & Trad, 2010).

  1. **Common reference**: this method uses one common reference for all electrodes. The position of this reference should be situated at a large distance from all electrodes. Using one of the EEG electrode as reference, such as the central Cz electrode as in the Common Vertex Reference, is discouraged as this reference also contains part of the signal. A very common method is to use as reference the average between two electrodes situated on the earlobes or on the mastoids. This position is situated at a larger distance from the electrodes and contains thus less signal. The use of two electrodes as a symmetrical reference avoids biasing recordings toward activity in one hemisphere.
  2. **Average Reference**: this method consists in using the average of all electrodes as reference. This requires a high number of electrodes and would ideally require recordings from all around the head.
  3. **Current Source Density**: the method of Current Source Density is based on the idea that currents are reference-free. The method consists in estimating these currents from the measured voltages. Once

these reference-free currents are computed, associated source voltages are derived from them, independently of any reference (Hjorth, 1975). This method, although based on an interesting physical principle, suffers from practical limitations such as for example the electrodes that must be situated in a plane at equal distances from each others.

Note that the signal do not especially have to be recorded with respect to the chosen reference. It can be recorded with respect to another reference and be rereferenced during the processing.

- **Temporal filtering**:
  Aside from the continuous filtering done in hardware by the acquisition device, the signal is mostly processed in software using digital filtering techniques. There are two main types of digital filters used in the field of BCI and more generally in the biomedical sector (Tompkins, 1993).

  1. **Finite Impulse Response (FIR) Filter**: FIR filters are not recursive, which means that their output only depends on the present and past inputs without any feedback. The main advantage of this non recursive filters is that they have no other poles than the ones in zero and are thus inherently stable. An other important feature of FIR filter is that it is easy to implement with a phase response proportional to the frequency. This kind of filters are called linear phase filter and are of high interest in the biomedical fields as they allow to keep the distortion of the data very low, which is very important when dealing with pattern recognition. The main disadvantage with respect to the Infinite Impulse Response is that the attenuation outside de band-pass is smaller. To counteract this drawback, FIR are often of much higher order, and are therefore more computationally demanding (Tompkins, 1993).
  2. **Infinite Impulse Response (IIR) Filter**: The output of an Infinite Impulse Response filter depends on the present and past inputs but also on the past outputs. In this case, problems of stability can occur. Moreover, IIR filters do not have a linear phase response. Their main advantage is that the rolloff can be sharper than for FIR filters (Tompkins, 1993).

- **Spatial filtering**: Next to the temporal behavior of the signal, its spatial distribution may also require filtering techniques in order to enhance the signal of interest. The simplest spatial filtering consists in selecting the electrodes based on a prior knowledge of the signal. In certain application, it is possible to select the electrodes based on the signal itself through

the **Common Spatial Pattern** method (Müller-Gerking, Pfurtscheller, & Flyvbjerg, 1999). Altough Common Spatial Pattern can be used as a spatial filter only, its use is most of the time coupled with the generation of the input vector of the classifier. Therefore, Common Spatial Pattern will be described extensively in the section 2.2.3 about feature extraction.

Apart from the selection of the electrodes, their also exist methods that aim at minimizing the volume conduction effect that has as consequence that electrodes do not only record the underlying neurons but also the electric activity around neighbor electrodes. This is the case of the **Surface Laplacian**. Decreasing the volume conduction effect improves the spatial resolution of the signal. The local Surface Laplacian consists in substracting from each electrode the signal of the adjacent electrodes. This acts as a high-pass spatial filter (Al-ani & Trad, 2010).

2.2.3 Feature extraction

The third building block of a BCI is the feature extraction. This step aims at providing a vector of features to the classifier. Various feature extractions methods can be used. However, when dealing with brain rhythms, one method has emerged and proved its efficiency: **Common Spatial Pattern (CSP)**. Consequently, this chapter describes in detail this feature extraction method.

The use of Common Spatial Pattern (CSP) in BCI context was suggested for the first time in (Müller-Gerking et al., 1999). The advance of CSP on other processing methods can be demonstrated by looking at its performances in the BCI competitions starting from the third one where in all but one case where oscillatory features were available, the winning method used CSP or variants of CSP (Blankertz et al., 2006).

Common Spatial Pattern computes weighting coefficients for each electrodes in a way that maximizes the difference between two classes (Müller-Gerking et al., 1999). These coefficients are directly derived from the data without any prior knowledge of neurological phenomena. However, it has been shown that the computed coefficients reflect the known Event-Related Desynchronization (ERD) described in section 2.2.2 . A spatial pattern, as described in (Müller-Gerking et al., 1999), is a sample containing the amplitudes of the signal at each electrode at a particular time. A set of patterns contains thus the amplitudes of the signal at each electrodes for several samples. Two different sets of patterns are obtained by concatenating the epochs corresponding to the two classes. The CSP algorithm takes as input these two sets of patterns and computes the directions in the pattern space that discriminate the best the two classes.

Common Spatial Pattern is illustrated in figure 2.6. The signal is recorded from the two electrodes X_1 and X_2. A pattern contains thus the amplitude of the signal at these two electrodes at a particular time and can be plotted as a single point in the 2D pattern space. Plotting several patterns leads thus to the point cloud on the left-hand side of figure 2.6. Red crosses correspond to the set of patterns associated to one class while blue circles corresponds to the set of patterns associated to the other class. The directions computed by the algorithm are shown in dashed lines. The coordinates of each pattern along the red direction will be really close to zero for the blue class and more widely spread for the red class. This coordinate is the coordinate S_2 on the right-hand side of figure 2.6. Coordinate S_1 corresponds to the coordinates of the patterns along the blue direction. The directions, being in the pattern space, can be expressed as linear combinations of the unit vectors of the space. As these unit vectors are given by each electrode, the directions are linear combination of the electrodes and the coefficients constitute the weighting coefficients applied on each electrode. In the example of figure 2.6, the red direction will have a bigger weighting coefficient for electrode X_1 than for electrode X_2 and inversely for the blue direction.

The mathematical development can be found in (Müller-Gerking et al., 1999).

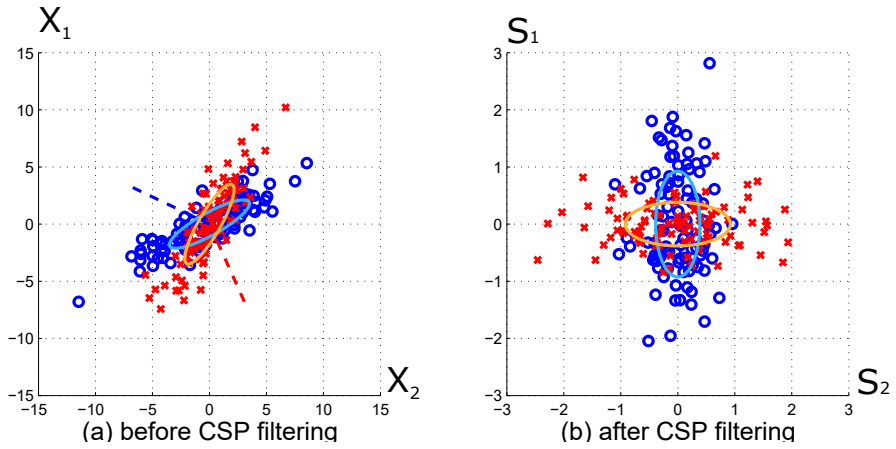

Figure 2.6: The left-hand side figure shows raw samples of data measured at two electrodes X_1 and X_2 for two different classes. The CSP algorithm computes the directions (shown in dashed lines) that minimize the variance of one class while maximizing the variance of the other class. The right-hand side figure shows the point cloud obtained after CSP filtering. S_1 and S_2 are the coordinates of the points taken along the blue direction and the red one respectively. The directions computed in this pattern space are linear combinations of the electrodes, which gives the weighting coefficients applied to each electrodes. In this example, the red direction will have a bigger weighting coefficient for electrode X_1 than for electrode X_2 and inversely for the blue direction (Blankertz et al., 2008).

After projection onto S_1 and S_2, the variance along the first dimension is maximal for one class and minimal for the other and reversely along the second direction. These variances along the computed directions are chosen as the features to be extracted. Doing so, recordings from a possibly very high number of electrodes are reduced to a low dimensional vector containing variances of the signal along the pairs of directions. The number of pairs of directions can theoretically be chosen equal to maximum half the number of electrodes. However, only a few pairs are typically sufficient for the discriminative task (Müller-Gerking et al., 1999). The dimensionality of the signal is thus considerably reduced.

As it was already mentioned, the CSP method reflect the changes in brain rhythms. This is illustrated in figure 2.7. This figure shows the first and second most discriminating patterns for the distinction of left finger movement from right finger movement obtained after bandpass filtering of the signal between 8 and 30Hz. The most discriminating pattern for the movement of left finger shows higher amplitudes around electrode C3 than around electrode C4, which is in agreement with the desynchronization happening in the opposite part of the motor cortex. For right finger movement, the reverse phenomenon is observed.

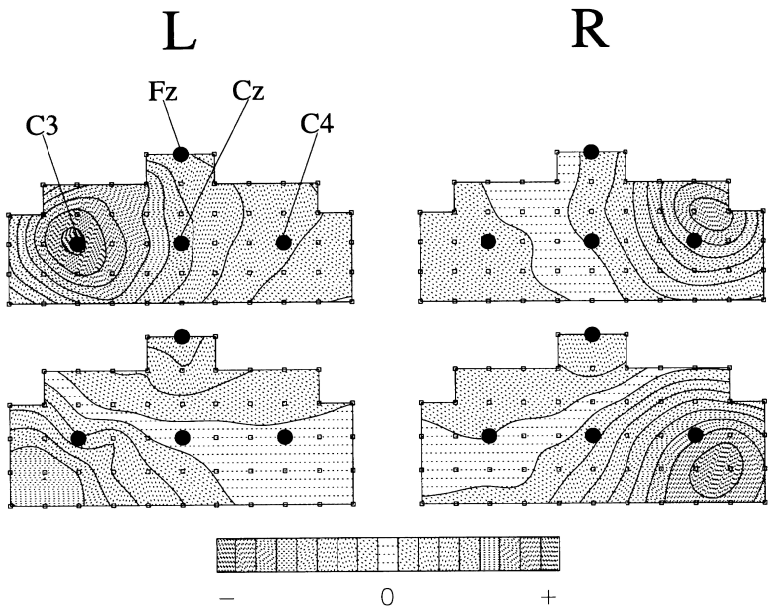

Figure 2.7: The patterns computed by the CSP feature extraction method reflect the changes in μ rhythm that happen during motor imagery (Müller-Gerking et al., 1999).

One advantage of CSP is that the weighting of the electrodes is done based on the signal itself. Consequently, if the position of the electrodes is not exactly the theoretical one, the algorithm will compute the weighting coefficients accordingly

without any loss of performance. Moreover, as the coefficients are computed based on the variance of the signal, they can theoretically enhance any possible neurological phenomena causing any variance in the signal. The consequent drawback is that artifacts can also be amplified if they are not properly filtered.

Once the coefficients are computed, they are applied to incoming data by simple scalar products. Hence, the method is not computationally demanding and is well suited for online data processing (Müller-Gerking et al., 1999).

The success of CSP-based methods had a promoting effect such that numerous variants of CSP analysis were developed as the Spectrally weighted Common Spatial Pattern (SpecCSP) (Tomioka et al., 2006) or the Filter Bank Common Spatial Pattern (FBCSP) (Ang, Chin, Zhang, & Guan, 2008) that add frequency features to the algorithm.

2.2.4 Classifier

After the feature extraction, generated vectors of features must be classified. This section summarizes the State of the Art of classifiers used in the BCI field.

There exist numerous types of classification algorithms. (Lotte, Congedo, Lécuyer, & Lamarche, 2007) provides an overview of the different classifiers used in EEG-based BCI research and describes their main properties.They can be grouped in five classes of algorithms which are described in the first part of this section. In the second part, it will be demonstrated that a simple linear classifier such as Linear Discriminant Analysis is particularly well suited for the classification of the vector generated by the Common Spatial Pattern method.

Classes of classifiers

Linear classifiers Linear classifiers are the most popular algorithms in the field of BCI. Their low complexity makes them less sensitive to small variations of the training set, which makes them more stable. They are only able to classify single feature vector, which means that they can not handle temporal information. Classifiers without temporal information are called static classifier. The most known linear classifiers are Linear Discriminant Analysis (LDA) and Support Vector Machine (SVM) (Lotte et al., 2007).

Neural Networks (NN) Neural Networks are the second most used classifiers in BCI applications. The main difference with the previous type of classifiers is that their structure allows them to perform nonlinear classification. Their higher complexity makes them unstable, which means that small changes in the training set can results in non negligible losses of performance. This complexity

also allows some NN to handle sequences of feature vectors rather than only one, which allows to add temporal information to the classification. These classifiers are said to be dynamic. The most widely used Neural Network in the BCI field is the MultiLayer Perceptron (MLP) (Lotte et al., 2007).

Nonlinear Bayesian classifiers Nonlinear Bayesian classifiers also perform nonlinear classification. The main difference with the previous classes of classifiers is that they are generative. Generative classifiers classify feature vectors by computing the likelyhood of each class and selecting the class with the highest probability. Previous classifiers, which are dicriminative classifiers, learn the way of discriminating classes and classify feature vectors directly. Generative classifiers allow to reject uncertain data in a more efficient way. The most known Bayesian classifiers are the Bayes quadratic and the Hidden Markov Model (HMM) (Lotte et al., 2007).

Linear Discriminant Analysis

The feature extraction method associated with the CSP algorithm produces low dimension normal distributed vectors of features that can be classified using simple linear classifier. Linear Discriminant Analysis (LDA), also called Fisher's LDA, is used to separate different classes, assuming normal distribution of the data and equal covariance matrix for both classes, which is obtained by taking the logarithmic value of the feature vectors (Müller-Gerking et al., 1999). For a two-class problem, only one hyperplane is needed, and the translation of the feature vector is given by the side of the hyperplane on which this vector is (figure 2.8). This separating hyperplane is obtained by seeking the projection that maximizes the distance between the two classes means and minimizes the interclasse variance.

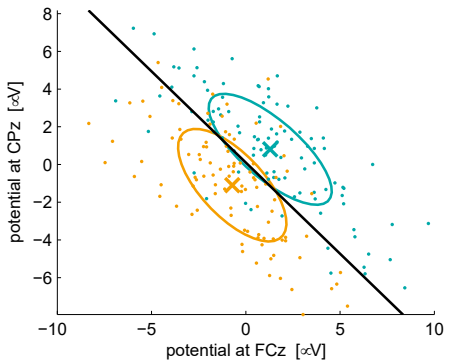

Figure 2.8: LDA consists in finding a hyperplane that maximizes the distance between the classes means and minimizes the interclasse variance. (Blankertz et al., 2011)

LDA has low computational costs, is simple to use, very robust and provides good results in most of the cases (Lotte et al., 2007). It gives bad results with nonlinear data.

Evaluation method

There are numerous methods that can be used to evaluate the performance of a classifier. (Schlogl, Kronegg, Huggins, & Mason, 2007) reviewed 19 different criteria. The most common one is the accuracy which is equal to the ratio of correct predictions divided by the total number of predictions. For a two-class problem, one defines true positives, true negatives, false positives and false negatives according to the correct or incorrect occurrence or absence of an action. When controlling a robotic hand, the incorrect occurrence of movement, or false positive, is very critical and must be avoided as much as possible.

Classifiers are most of the time evaluated by cross-validation. This consists in dividing the data set in several segments, train the classifier based on some of the segments and test in on the remaining segments. This is repeated several times using different segments for the training and the testing. The average accuracy is then computed. Because the training and the evaluation are done on the same data set, accuracy obtained by cross-validation is sometimes called offline accuracy. Classifiers should always be tested on a different data set to be validated. This is called online accuracy.

2.2.5 Feedback

BCI training have evolved from operant conditioning, where the subject had to learn producing the right brain patterns to control a predefined classifier, to machine learning where the classifier learns from the subject. Consequently, recent studies in the field of BCI mostly focus on improving the signal processing methods, the feature extraction and the classification, neglecting the importance of human learning mechanisms (Lotte, 2012).

Current approaches mostly provide a simple visual feedback under the form of a moving bar. There are many concerns about this kind of feedback, the most important being that it indicates if the user is performing well or not but do not give him any explanation on how he could improve. Alternative approaches exist and are partially reviewed in (Lotte & Jeunet, 2015). For example, Showing the user a real-time topographic image of his brain activation could help him in activating the right cortical zone in motor imagery-based BCI for example. Other approaches investigate the influence of biased feedback such as only providing a

feedback when the subject is doing well, or artificially increase the performance of the BCI to make the subject believe he is improving.

For BCI used in motor applications, having a feedback related to the motor task performed may have a promoting effect. In (Braun, Emkes, Thorne, & Debener, 2016), it was shown that the use of a feedback signal that closely resembles the mental task performed may help to embody the feedback signal into the one's body scheme and improve neurofeedback task-performance.

2.3 Existing tools

2.3.1 Hardware

There are numerous equipment available on the market for measuring the EEG activity. Some are used for medical purposes, others for research. More recently, open source headsets have been developed for personal use. This thesis being done in collaboration with the Consciousness, Cognition & Computation Group (Co3) from the Université Libre de Bruxelles, a BioSemi ActiveTwo was made available for the present work. The specifications of this device can be found in appendix A. Two other general purpose headsets were available too: the Emotiv EPOC and the OpenBCI (Durka et al., 2012). Figure 2.9 shows the three different devices.

(a) BioSemi (b) Emotiv EPOC (c) OpenBCI

Figure 2.9: Existing hardware

Table 2.1 shows a comparison of the specifications of each acquisition system. The Emotiv EPOC and the OpenBCI have the advantage of being wireless and have a reduced setup time due to their lower number of electrodes. The OpenBCI presents the lowest setup time thanks to its dry electrodes. The absence of electrodes around the motor cortex area is a critical drawbacks for the Emotiv

EPOC. Although the OpenBCI allows having electrodes around the motor cortex area, it was demonstrated in (Suryotrisongko & Samopa, 2015) that it did not offer an optimum placement for motor imagery tasks. The BioSemi presents a longer setup time but its 64 electrodes offer a much higher spatial resolution. The higher sampling rate and the higher resolution are also much better than the one of the two other headsets. The higher capability of the BioSemi with respect to the Emotiv EPOC is demonstrated in (Nijboer, van de Laar, Gerritsen, Nijholt, & Poel, 2015).

	BioSemi ActiveTwo	Emotiv EPOC	OpenBCI
Number of electrodes	$64 + 8$	14	8
Electrodes on motor cortex	yes	no	yes
Type of electrodes	wet electrodes	wet electrodes	dry electrodes
Sampling rate	up to $16,384Hz$	up to $256Hz$	$250Hz$
Resolution	24 bits LSB $= 31.95nV$	14 bits LSB $= 0.51\mu$V	24 bits
Supply	battery	battery	battery
Connectivity	USB2	wireless	wireless
Cost	$> 30000e$	$799\$$	$\sim 850\$$

Table 2.1: The BioSemi ActiveTwo available thanks to the Consciousness, Cognition & Computation Group (Co3) from the Université Libre de Bruxelles has far better performances.

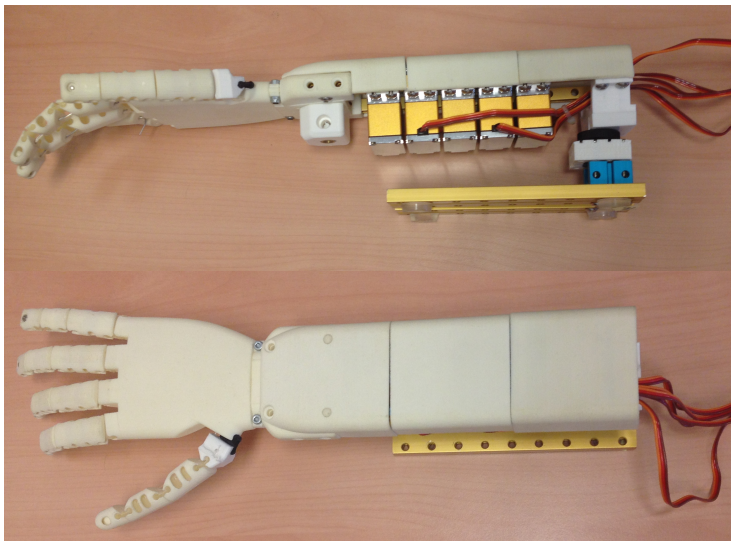

Figure 2.10: 5 servo-motors allow to bend the 3D-printed fingers independently in a very fast way (De Beir et al., 2014)

Next to the acquisition device providing the input of the BCI, the hardware to which the output is sent is also important. As explained in section 2.2.5, most

research are sending the output to a visual display. Regarding the neuroscientific context behind this thesis, it was important to have an output that could be identified as part of the subject's body. In (Alimardani, Nishio, & Ishiguro, 2016), this is achieved by reconstructing the hand of the subject in a virtual environment. For the present work, the robotic hand designed in (De Beir et al., 2014) was used. This artificial hand was designed specifically for the Rubber Hand Illusion (see section 1.1). 5 servo-motors allow to bend the 3D-printed fingers independently in a very fast way. The hand is controlled by an arduino that can receive commands through a serial communication. This robotic hand is shown in figure 2.10

2.3.2 Software

The number of available software for BCI research is huge. Here are a non exhaustive list containing the most important ones:

- EEGLAB and BCILAB(Delorme & Makeig, 2004; Kothe & Makeig, 2013)
- FieldTrip (Oostenveld, Fries, Maris, & Schoffelen, 2011)
- OpenVibe (Renard et al., 2010)
- BioSig (Schlögl & Brunner, 2008)

OpenVibe is a very interesting software for newcomers in the field of BCI as it offers the possibility to design BCI's by dragging and dropping blocks in a visual scenario designer. It also has the advantage of working independently of any costly software. However, the number of implemented blocks is limited and implementing one's own blocks requires more programming skills.

EEGLAB is a matlab toolbox designed for offline analysis of EEG signals. BCILAB is an extension of EEGLAB allowing to design BCI's and run online applications. FieldTrip and BioSig are matlab toolboxes too. All these toolboxes share some of their functions, which makes it not to complicated to exchange data from one to another. EEGLAB and its extension BCILAB are targeting a wider audience. They propose a graphical interface in order to get started with the structure of the toolbox, while calling functions from the command line or from a script is possible too. Numerous approaches are implemented including more recent variants of Common Spatial Pattern.

For these reasons, EEGLAB and BCILAB were chosen as environment to develop the Brain Computer Interface. These toolboxes use an external protocol called Lab Streaming Layer (LSL) in order to receive signals from the EEG or from other devices, and to send data such as markers for the training of the

classifier. LSL is a layer in charge of the synchronization of the streams that are sent on it. Various applications can then connect to the layer in order to add a new stream or to connect to an existing one and start copy it to disk, display it on screen, or process it for class prediction.

2.4 Summary and research objectives

This chapter reviewed the State of the Art in the field of Brain Computer Interface. First, the working principle of a BCI was described in section 2.1. After that, section 2.2 reviewed every aspects constituting this technology. Finally, section 2.3 gave an overview of the different hardware and software tools available.

Every aspects detailed in the present chapter are grouped together in chapter 3 in order to implement the Brain Computer Interface needed by the Consciousness, Cognition & Computation Group (Co3). Being implemented in this particular neuroscientific context, the BCI has to fullfill specific requirements.

The task studied by the Co3 research group is a binary task where participants must be able to control the opening and closing of the robotic hand. Inducing the Rubber Hand Illusion requires particular specifications. First of all, the response of the Brain Computer Interface must be as fast as possible since an oversized delay kills the illusion (Shimada, Fukuda, & Hiraki, 2009). Second, the prediction of the Brain Computer Interface must be as accurate as possible. In particular, the false positive have to be avoided as much as possible. Next to that, the time needed in order to get in control of the BCI is also critical. Indeed, the experiments foreseen by the Co3 research group do not plan months of training to be able to modulate one's brain waves. Moreover, training sessions are expected to be exhausting for the participants. Hence, the implemented BCI should be trained in a very limited amount of time. Additionally, the BCI should work for as many users as possible to avoid waste of time and of money. Finally, functionality is a crucial point for the neuroscientific researchers to be able to use it and modify it in the future.

The Brain Computer Interface will attempt to meet these requirements while making use of the available tools: the BioSemi ActiveTwo as input, and the previously designed robotic hand as output (see section 2.3.1). The translation from the former to the latter will be implemented in Matlab using BCILAB (see section 2.3.2).

Chapter 3

Implementation of the Brain Computer Interface

This chapter describes the selection of the method and the way it is implemented. First, requirements of section 2.4 are restated in terms of technical requirements. Three methods are then proposed based on the State of the Art and on these requirements. After that, these methods are tested on data sets available from the previous BCI competitions. Results are compared to those obtained by the research centers participating to this competition and a final method is selected. Once this method is selected, the complete setup that will be used for the neuroscientific experiments is described, as well as the architecture of the algorithm.

3.1 Technical requirements

To be able to implement the BCI in an optimal way, it is important to determine in advance the context in which it will be used. General requirements were already mentioned in section 2.4. After discussion with the Consciousness, Cognition & Computation Group (Co3) from the Université Libre de Bruxelles, the following elements were decided:

- Number of classes:
  The BCI must be able to discriminate 2 different classes: right hand versus rest.

- Accuracy of the classifier:
  In (Evans, Gale, Schurger, & Blanke, 2015), only the participants with an accuracy above 75% were allowed to perform the neuroscientific experiment. It was decided to keep the same threshold.

- Time response of the BCI:
  The delay induced by the BCI must be smaller than $1s$ to avoid killing the illusion of control.

- Total training time:
  It was decided to limit the total training time to $30min$ since it is only a calibration before the real experiment.

- Number of participants:
  The objective was to get at least half the participant in control of the BCI and be able to perform the neuroscientific experiment.

3.2 Method selection

As explained in section 2.2.3, Common Spatial Pattern (CSP) has become the reference in Brain Computer Interface based on the activity in the μ band. Several variants of CSP were developed through years. In the present work, the results obtained using three CSP variants are compared. BCILAB was chosen as toolbox for implementing the BCI (see section 2.3.2).

3.2.1 Preselection of methods

The three variants of CSP that were preselected are the following:

1. Common Spatial Pattern (CSP)
2. Spectrally weighted Common Spatial Pattern (SpecCSP)
3. Filter-bank Common Spatial Pattern (FBCSP)

The following parameters were selected:

- **Processing**
  - **Electrodes**:
    The choice of the electrodes depend on the set of available electrodes. In order to minimize to influence of artifacts, the electrodes positioned on the motor cortex are chosen.
  - **Rereferencing**:
    When reference electrodes are available, the signal is rereferenced to these reference electrodes.

- **Temporal filtering**:
  The temporal filtering is done in a different way for each of the methods:
  - **CSP**: As classical CSP is known to work well on a broad frequency range (Müller-Gerking et al., 1999), the signal is bandpass filtered between 7 and $30Hz$. A Finite Impulse Response filter was chosen because of its inherent stability (see section 2.2.2).
  - **SpecCSP**: altough Spectrally weighted CSP automically weigths frequency bands relevant for the discrimination of the classes, it also requires a wide bandpass prefiltering (Tomioka et al., 2006). The signal is also bandpass filtered between 7 and $30Hz$ using a Finite Impulse Response filter.
  - **FBCSP**: In the Filter Bank CSP method, the signal is filtered in different frequency bands before CSP is applied to each of this band. Two bands were chosen: $8-12Hz$ corresponding to the μ band and $13-30Hz$ corresponding to the β band. The method then automatically weights the results in these two bands for the discrimination of the classes.

  It was important here to apply the different methods to the same broad frequency range in order to be able to conveniently compare the results afterwards.
- **Spatial filtering**:
  As it was detailed in the section 2.2.3, Common Spatial Pattern is used as a spatial filtering technique. The principle is the same for the two variants. The only parameter here is the number of pairs of directions on which the spatial projection is performed. As only a few pairs of directions are necessary, a single pair of directions was chosen in order to minimize the computation time.

- **Feature extraction**:
  The feature vectors are obtained by the projection of the signal onto the directions computed by the CSP, the SpecCSP or the FBCSP method.

  A very important parameter here is the length of the window from which the feature vector is extracted. A very short window allows to have faster transition of the output of the BCI because the signal of interest is not averaged over time. However, short windows also increases the risk of mis-classification and wrong output because the variance of the signal is computed based on less data. In order to study the influence of this parameter, three window lengths were studied: $1s$, $2s$ and $3s$.

- **Classifier**:
  The classifier used in each method is Linear Discriminant Analysis (see section 2.2.4).

  During the training sessions, most of the time the participants are asked to perform the tasks during a longer period than the length of the window used for feature extraction. In order to train the classifier, the algorithm developed in this thesis uses a sliding window in order to find the window producing the best results. The idea of this moving window came from the fact that some subjects may have different reaction time when being presented visual stimuli. Hence, the part of the signal with the most interesting content may shift from one subject to the other. Three different steps were used to slide the window in order to study the influence of this parameter: $0.1s$, $0.2s$ and $0.5s$. The smaller the step, the better the results as the position of the window can be tuned more precisely. However, this is done at the cost of a longer computation time as the classifier is trained for each position before selecting the best one.

  The last parameters that was studied is the handling of several training sessions. On one hand, the participant is supposed to improve its control over the BCI. Hence the classifier trained on the last training session should perform best. On the other hand, the accuracy of a classifier increases when it is trained with a bigger amount of data. In that case, concatenating the data from all training sessions should give better results.

3.2.2 Test on data sets from BCI competitions

The three methods presented in section 3.2.1 were applied to publicly available data set 2b from the BCI competition IV: *Session-to-Session Transfer of a Motor Imagery BCI under Presence of Eye Artifacts*. Using these data allowed to compare the results obtained with the methods presented here with those obtained by the competitors. Indeed, methods can properly be compared only if they are applied to the same data.

This data set comes from (Tangermann et al., 2012). It contains the recordings of 5 sessions from 9 subjects. The 3 first sessions are provided with the labels in order to train the classifier, while the 2 last sessions are used in order to evaluate the classifiers. Each session contains 120 trials divided in 2 classes: motor imagery of left hand and motor imagery of right hand. Each trial starts with a fixation cross. After $3s$, a visual clue presenting an arrow pointing to the left or to the right is presented during $1.25s$. The visual clue is followed by $4s$ during which motor imagery of the corresponding class is performed. The trial ends with a break of between 1.5 and $2.5s$. The complete timing scheme of the

paradigm is illustrated in figure 3.1.

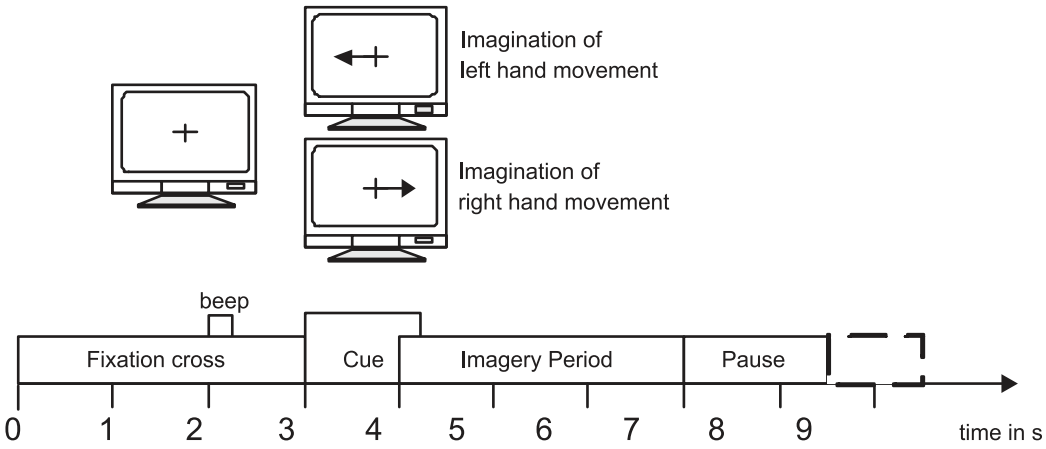

Figure 3.1: Cued paradigm used in the data set IIb of the BCI Competition IV (Leeb et al., 2008)

The EEG signal is recording using 3 electrodes over the motor cortex at C3, Cz and C4, with a sampling rate of $250Hz$. The reference of the signal is the electrode Fz and is not provided. The evaluation criteria is the kappa value. The kappa coefficient is 0 if there is no correlation between the predicted classes and the real ones, and 1 in case of perfect classification (Schlogl et al., 2007). A more complete description of the data set can be found in (Leeb et al., 2008).

The first important results concern the session-to-session transfer challenge. The offline accuracy of the classifiers, obtained by cross-validation, reaches its maximum for the session 3 (see figure 3.2). This is expected since the participants are improving. The offline accuracy obtained for the model computed based on all sessions concatenated seems to correspond to an average of the offline accuracy computed for each session separately. Note that these results are obtained by averaging the results across subjects and across methods, for every possible combination of parameters. Therefore, the standard deviation is high and this first observation may not be respected for every single combination of parameters and subjects. Interestingly, the model that performs the best on the test data sets is the model computed from all concatenated training sessions. A possible explanation is that this model being computed from a bigger amount of data, it is more robust and performs thus better on new data. Therefore, it was chosen to always use every data sets available as source data for the training of the classifier and not only the data from the last training session. When evaluated at each time point, the accuracy of the classifier decreases significantly. However, the cumulative model still performs better than the other models. Lots of studies only consider the first evaluation method, which consists in giving one

prediction for each trial, at the marker indicating the beginning of the imagery period. However, in online application, the second prediction method is much more realistic.

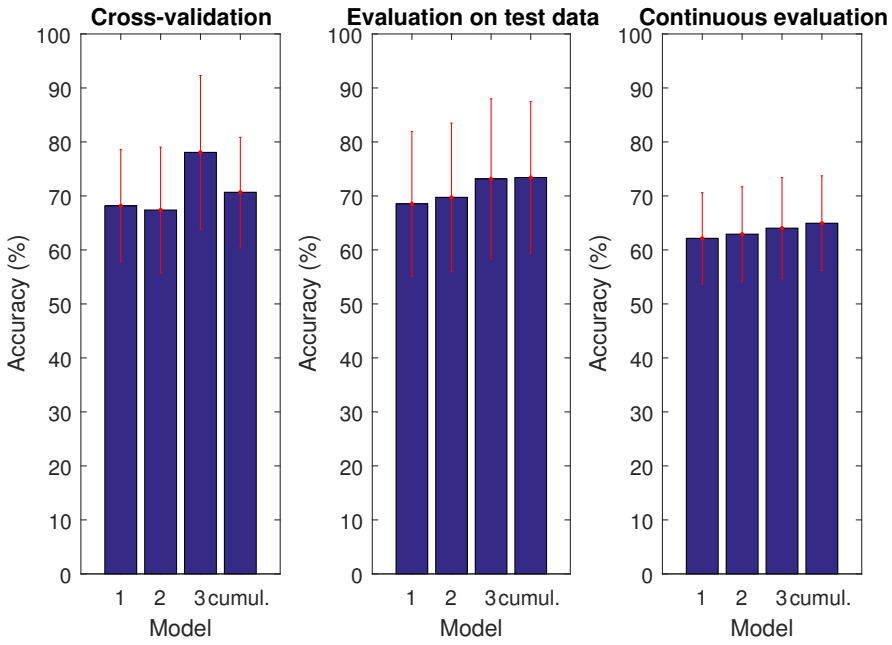

Figure 3.2: The session from which the model is computed influences a lot the performance of the classifier. The offline accuracy obtained by cross-validation is far better for the model trained on session 3. However, being computed from a bigger amount of data, the cumulative model is more robust and performs better online on a new data set. The difference is more visible when the accuracy of the model is evaluated at each time point and not only at the markers.

The next parameter that was studied was the length of the window. Figure 3.3a shows the results averaged across participants and across methods for the cumulative models only. Results obtained with one prediction by trial are better for the window of $2s$. When considering continuous predictions, the difference with the window of $1s$ is much smaller, which could be explained by the fact that for the latter, the loss in term of accuracy is compensated by the faster response. As the difference is very small, the faster response given by the $1s$ window was chosen.

The influence of the sliding step was studied next. As mentionned in section 3.2.1, the lower this parameter the thinner the tuning of the classifier but the larger the computation cost. Results obtained when averaging across participants and across methods for the cumulative models using the selected window of $1s$, are shown in figure 3.3b. In continuous evaluation, the sliding step of $0.1s$ results

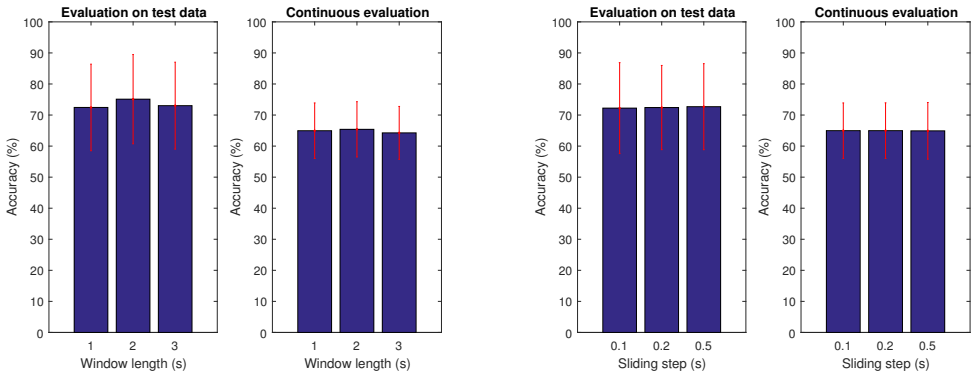

(a) Influence of the window length (b) Influence of the sliding step

Figure 3.3: The size of the window is a trade-off between the accuracy of the classifier and its responsiveness. Results being very similar in continuous evaluation, the shortest window of $1s$ was chosen. Concerning the size of the sliding step, the lower the size the thinner the tuning of the classifier but the larger the computation cost. The sliding step of $0.2s$ was chosen.

in an accuracy of $64.98\% \pm 8.93\%$, the sliding step of $0.2s$ in an accuracy of $64.98\% \pm 8.96\%$, and the sliding step of $0.5s$ in an accuracy of $64.91\% \pm 9.12\%$. The results using the step of $0.2s$ were as good as those using the step of $0.1s$, and slightly better than those using the step of $0.5s$. Therefore, the length of this sliding window was fixed to $0.2s$. However, the difference being very small, if the time needed in order to train the classifier is judged to be too long by the future experimenter, the length of this sliding window could be decreased with a negligible loss of performance.

Finally, the 3 variants of CSP are compared. Models were computed based on the cumulated sessions, with a window of $1s$ and the sliding step of $0.2s$ as just determined. Figure 3.4 shows the results obtained when averaged across subjects. In continuous evalution, CSP reached an accuracy of $64.76\% \pm 8.99\%$, SpecCSP an accuracy of $65.59\% \pm 9.48\%$ and FBCSP and accuracy of $64.58\% \pm 8.89\%$. FBCSP has a smaller average accuracy but also a smallest standard deviation which can be interesting to meet the requirements regarding the ratio of participants able to control the robotic hand. However, the difference between the different feature extraction methods are too small to be able to really conclude that one method is better than another. The choice of the method was then based on the literature. The winning team for the studied data set of the BCI competition IV used FBCSP. Moreover, they also performed best on a data set assessing a 4 classes motor imagery BCI (Tangermann et al., 2012; Ang, Chin, Wang, Guan, & Zhang, 2012), which could be interesting for future studies. Hence, the Filter Bank Common Spatial Pattern was chosen as feature extraction

method.

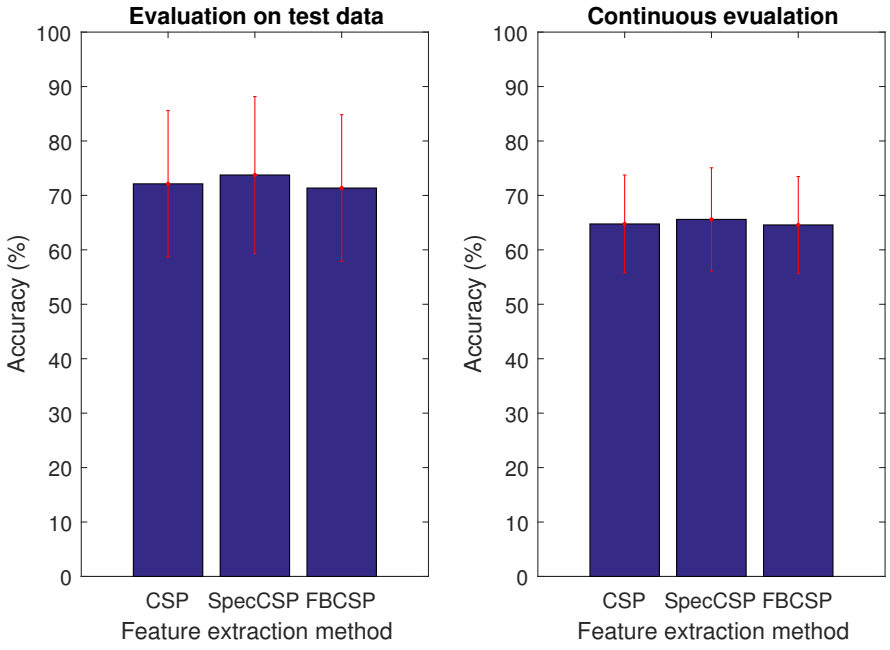

Figure 3.4: The accuracy obtained using SpecCSP as feature extraction method is slightly better. However, the difference between the results being very small, it was decided to select FBCSP because of its success in the litterature (Tangermann et al., 2012; Ang et al., 2012)

3.2.3 Summary and comparison

The final method used to train the model uses Filter Bank Common Spatial Pattern with 2 frequency bands: $8-12Hz$ and $13-30Hz$. The feature vectors are generated from windows of $1s$. The data from all training sessions are used as train data. During the training of the classifier, the algorithm uses a moving window with a sliding step of $0.2s$ to search for the best offline accuracy. Figure 3.5 shows the results obtained for each of the 9 subjects. Results are highly dependents on the subjects. When evaluated at each time point, the accuracy varies from 53.04% for subject 2 to 78.36% for subject 4. On the contrary, subjects perform similarly during the 2 test sessions.

Figure 3.6 details the results obtained for the best subject on his best test session. Figure 3.6a shows the patterns computed by the Filter Bank Common Spatial Pattern feature extraction method. The first row corresponds to the frequency band $8-12Hz$ and the second row to the frequency band $13-30Hz$. For each frequency band, a pair of patterns is computed. As described

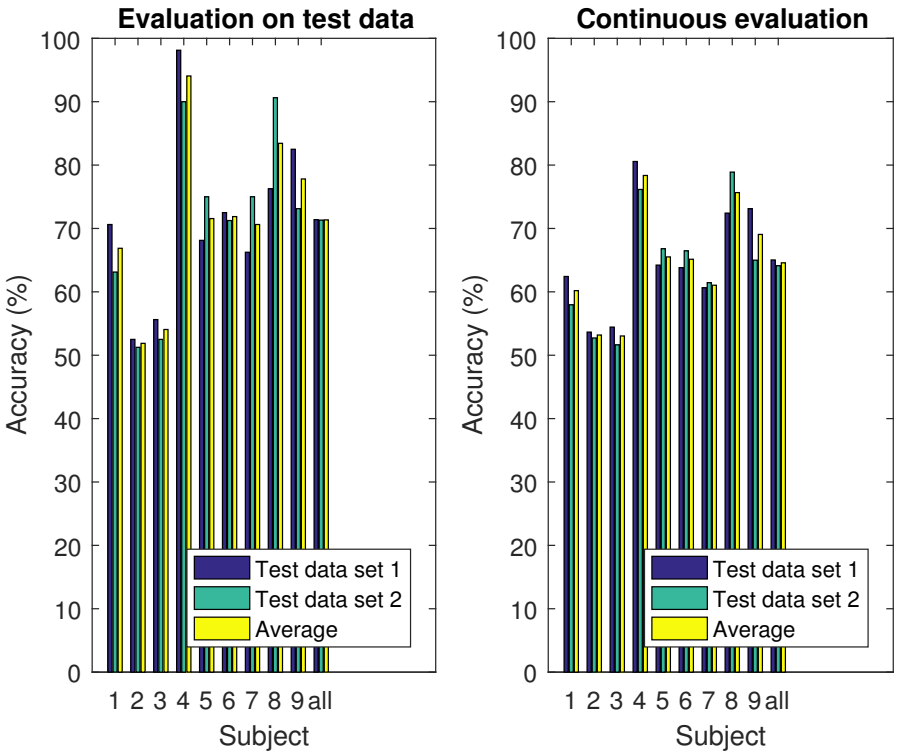

Figure 3.5: The accuracy varies a lot from one subject to the other. For subject 2 and 3, it barely exceeds chance level which is 50% for a 2 classes BCI. Only subjects 4 and 8 do exceed the level of 75% in continuous evaluation. Average accuracy is 71.35% for the evaluation at markers and 64.58% in continuous evaluation.

in section 2.2.3, each pattern defines a direction that maximize the variance of one class while minimizing the variance of the other class. As the Event-Related Desynchronization happens in the reversed part of the brain (see section 2.2.2), a movement of the right hand results in a reduced amplitude of the signal on the left electrode. Hence the amplitude and the variance of the signal from the right electrode are comparatively bigger and this electrode will be emphasized by the FBCSP method, which corresponds to the right upper pattern. The left upper one is the pattern which corresponds to the left hand movement. The pattern are scaled according to their importance in the discriminating task.

Figure 3.6b shows a section of the time course of the BCI output. This section was chosen because it matched well the expected value, but it is not the case for the complete signal. It has also to be remembered that these results are obtained for the best subject on his best session. Continuous BCI's, more often called asynchronous BCI's, remain a challenge (Tangermann et al., 2012).

The results obtained by the research centers participating to the BCI compe-

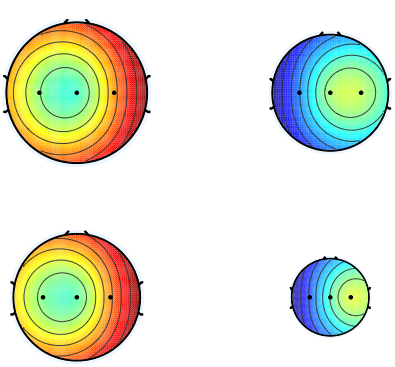

(a) Patterns computed by the Filter Bank Common Spatial Pattern during the training of the classifier. The first row corresponds to the frequency band $8 - 12Hz$ and the second row to the frequency band $13 - 30Hz$. The pattern are scaled according to their importance in the discriminating task

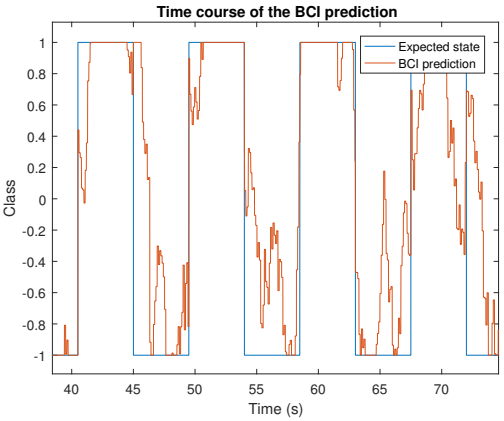

(b) Time course of the BCI output. Classes left hand movement and right hand movement are respectively represented by -1 and 1.

Figure 3.6: Results obtained for the subject 4 during his first test session.

tition are indicated in table 3.1. As already mentioned, the evaluation criteria is the kappa value, which is 1 for perfect classification and 0 if there is no correlation between the output of the BCI and the cue that is followed. The method implemented in the present work would have ranked 6th in the competition.

Part. ID	Mean	Subjects								
		1	2	3	4	5	6	7	8	9
ID-1	0.60	0.40	0.21	0.22	0.95	0.86	0.61	0.56	0.85	0.74
ID-2	0.58	0.43	0.21	0.14	0.94	0.71	0.62	0.61	0.84	0.78
ID-3	0.46	0.19	0.12	0.12	0.77	0.57	0.49	0.38	0.85	0.61
ID-4	0.43	0.23	0.41	0.07	0.91	0.24	0.43	0.41	0.74	0.53
ID-5	0.37	0.20	0.16	0.16	0.73	0.21	0.21	0.39	0.86	0.44
Thesis	0.29	0.20	0.06	0.06	0.57	0.31	0.30	0.22	0.51	0.38
ID-6	0.25	0.02	0.09	0.07	0.43	0.25	0.00	0.14	0.76	0.47

Table 3.1: Results shown in this table are the kappa values which are equal to 1 for perfect classification and 0 if there is not correlation between the predictions of the BCI and the expected state (Tangermann et al., 2012).

The data set of the BCI competition was assessing a BCI discriminating left hand versus right hand movement. However, it was interesting to see how

the selected method would perform on a right hand movement versus rest BCI. This was possible thanks to the markers present in the data set. Indeed, one marker indicated the beginning of each trial. Hence, from this marker to the one indicating the beginning of the cue, there were $3s$ of data during which the subject was not performing motor imagery.

The obtained results are shown in figure 3.7. Interestingly, the average across subjects and across sessions was slightly better than for the initial left hand versus right hand condition (64.67% against 64.58%). Moreover, the standard deviation also improved for the rest versus right hand condition (5.98% against 8.89%). However, these results require a deeper study since participants were not given proper instructions regarding what to do when the fixation cross is displayed and some of them were maybe already preparing the upcoming movement.

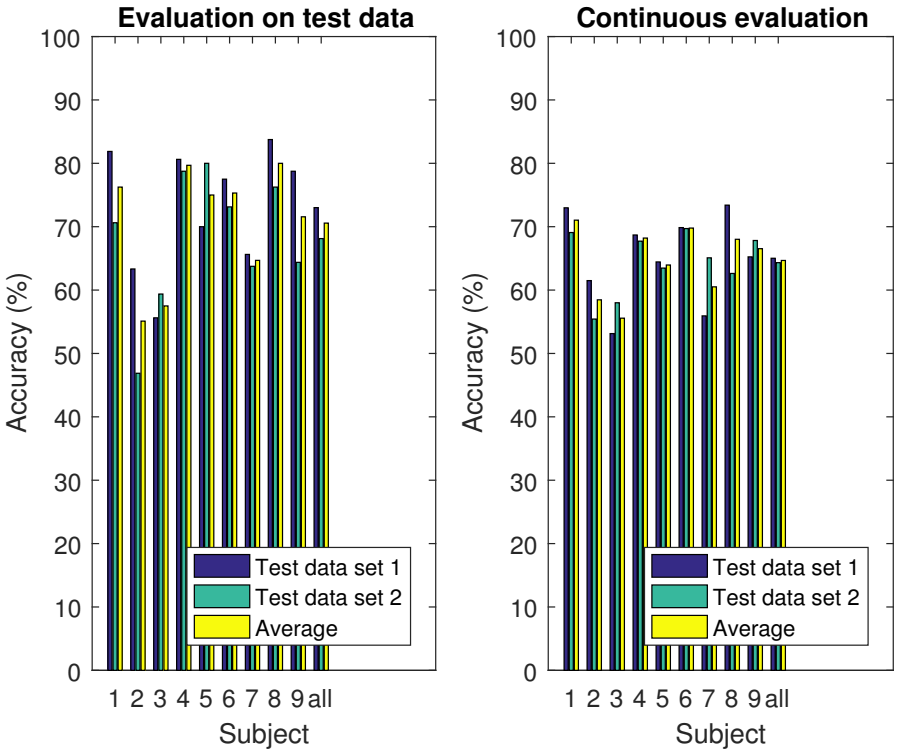

Figure 3.7: The accuracy varies a lot from one subject to the other. For subject 2 and 3, it barely exceeds chance level which is 50% for a 2 classes BCI. Only subjects 4 and 8 do exceed the level of 75% in continuous evaluation. Average accuracy is 71.35% for the evaluation at markers and 64.58% in continuous evaluation.

3.3 Description of the setup and of the architecture of the algorithm

The setup is shown in figure 3.8. The subject is sitting in front of a screen, with a keyboard and the robotic hand. His EEG activity is recorded at a sampling rate of $512Hz$ using a BioSemi ActiveTwo with 64 electrodes and 2 reference electrodes placed on the mastoids. The screen is used to display visual cues similar to those in figure 3.1. During the neuroscientific experiment, the subject has to use the keyboard to answer to some questions (see section 4.2). During this experiment, the robotic hand is placed on the keyboard such that it clicks on a key when activated. The experimenter controls everything from its computer. The EEG signals and the BCI predictions are displayed on his screen.

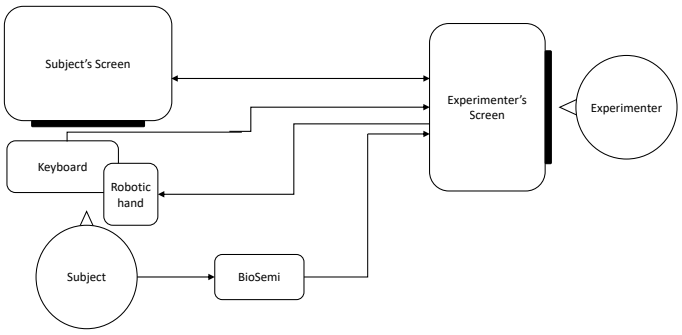

(a) Schematic setup

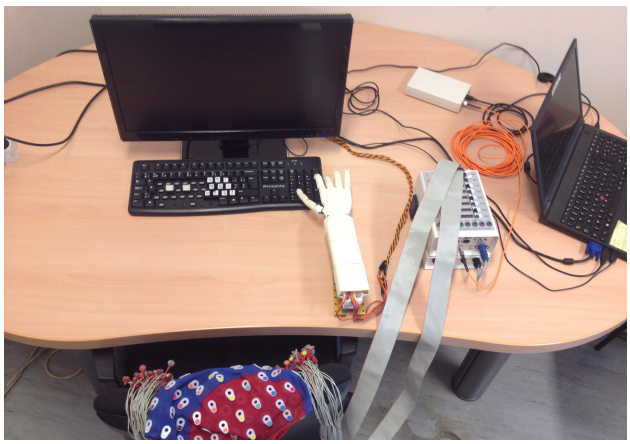

(b) Real setup

Figure 3.8: The subject is sitting in front of a screen, with a keyboard and the robotic hand. His EEG activity is recorded using a BioSemi ActiveTwo device. The subject's screen is used to display visual cues and instructions. The EEG signals and the BCI predictions are displayed on the experimenter's screen.

The objective of the neuroscientific research behind this work is to study the difference in terms of agency between an action performed using one's own hand or using an artificial hand controlled by the Brain Computer Interface (see section 4.2). Therefore, the experiment starts with a task $BCI\_0\_IB\_Basic.m$ performed without the BCI, and ends with the same task $BCI\_4\_IB.m$ performed with the BCI (see figure 3.9).

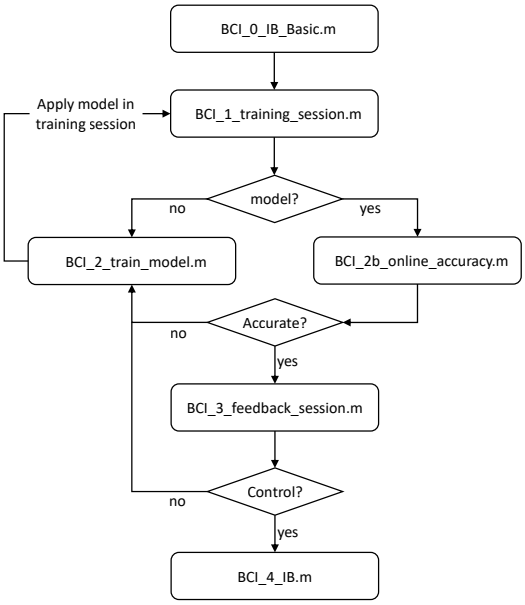

Figure 3.9: The training of the classifier is done iteratively starting from $BCI\_1\_training\_session.m$ to $BCI\_3\_feedback\_session.m$. Models are computed based on data recorded from the training sessions and are then tested online in a new session. When a sufficiently accurate model is obtained, the subject is given the possibility to it on the robotic hand in a free session. $BCI\_0\_IB\_Basic.m$ and $BCI\_0\_IB.m$ are linked to the neuroscientific experiment.

In between these two tasks, the subject and the classifier are trained in an iterative way. First, the subject has to follow a cued paradigm similar to the one presented in figure 3.1. $BCI\_1\_training\_session.m$ is in charge of loading the dependencies and run the paradigm on a separate screen for the subject. This visual paradigm is implemented using Psychtoolbox, a well-known matlab toolbox that is used a lot in neuroscientific research in order to present any kind of stimuli. The implemented cue is shown in figure 3.10. Each trial starts with a fixation cross displayed during 3 seconds. A red arrow pointing to the right is then superimposed to the cross during $2s$. After that, the cross and the arrow are removed from the screen during $2s$. Hence, each trial lasts $7s$. Training sessions consist in 20 consecutive trials. Markers are placed when the cross appears and when the arrow appears.

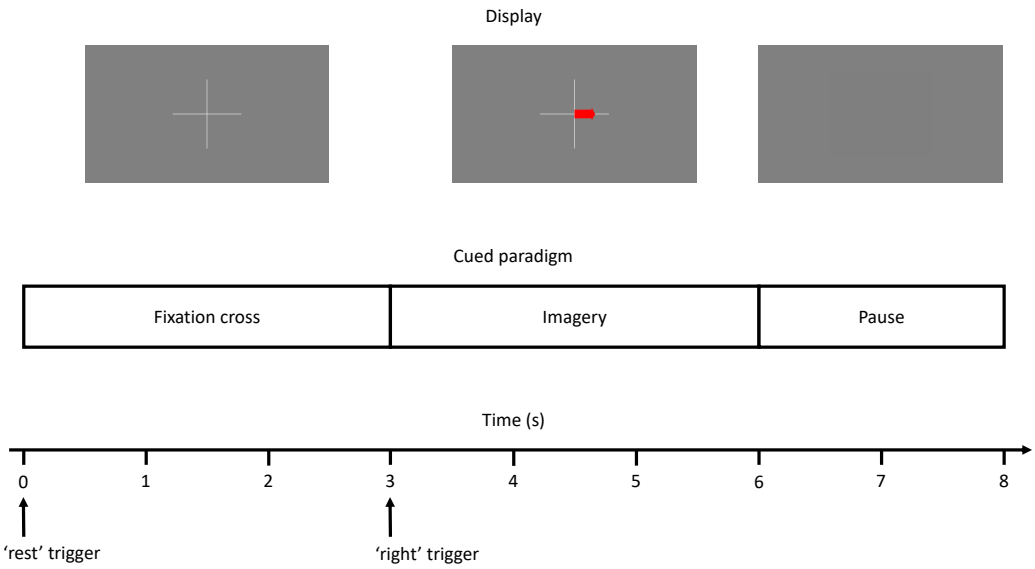

Figure 3.10: Each trial last $8s$ and is divided as illustrated. Markers 'rest' and 'right' are added to the recordings in order to train the classifier afterwards

The raw EEG signals are displayed on the experimenter's screen to allow him to monitor the experiment and give instructions to the subject if the task is not performed well. For example, in the figure 3.11 captured during the first training session, slow oscillations can be observed. This kind of oscillations are very typical of sweat artifact. Having this display allows the experimenter to be aware of this problem and react accordingly to reduce the temperature in the room.

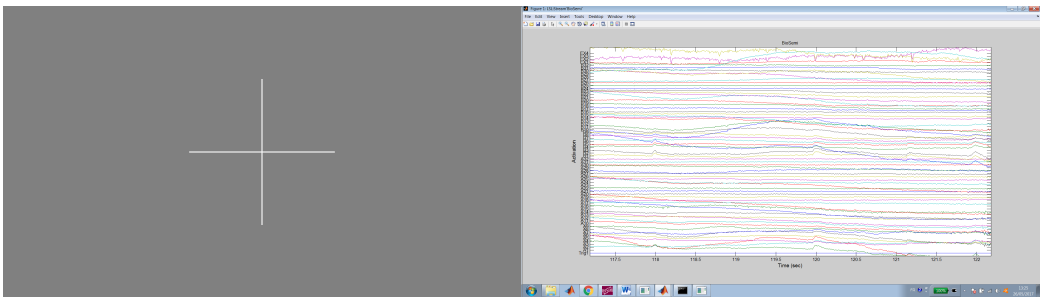

Figure 3.11: The real-time raw EEG signals of the subject are displayed on the experimenter's screen. Although brain features are most of the time not visible without signal processing, most artifacts are. Hence, the display allows the experimenter to identify them and react accordingly. For example, the present picture shows slow shifts due to sweat.

After the training session, a first classifier is then trained based on the markers indicating the period of imagination and of rest. The training of this model is

performed in the script $BCI\_2\_train\_model.m$. The accuracy obtained by cross-validation is displayed to the experimenter in the command line, as well as the patterns computed by Filter Bank Common Spatial Pattern that are plotted in a separate window. Figure 3.12 give an example of these patterns. The interpretation of those patterns is slightly more complicated than those of figure 3.6a since the class rest is not as well defined as the class left hand regarding the brain mechanism involved. However, the electrodes on the left motor area of the brain are expected to play a role in the discrimination since the right hand is still involved.

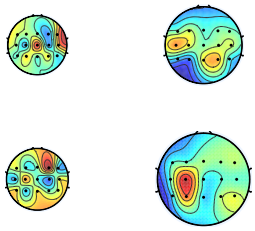

Figure 3.12: The patterns computed by the Filter Bank Common Spatial Pattern method are displayed on the experimenter screen to give him feedback about the participant's performance. In the example here, expected patterns are obtained.

After that, a second training session has to be done, during which the trained model is applied to the incoming data. This online prediction of the classifier is shown to the experimenter in real-time, allowing him to have a first idea of the accuracy of the classifier. Figure 3.13 captured during such a session illustrated this. Sweat artifact are still present but do not disturb the prediction of the BCI which was at high level at the moment of the capture, what corresponded to the expected state. The real-time prediction of the BCI is done every $10ms$ and oscillates between 1 and 2, 1 being the class 1 corresponding to rest and 2 being the class 2 correspond to the imagination of right hand movement.

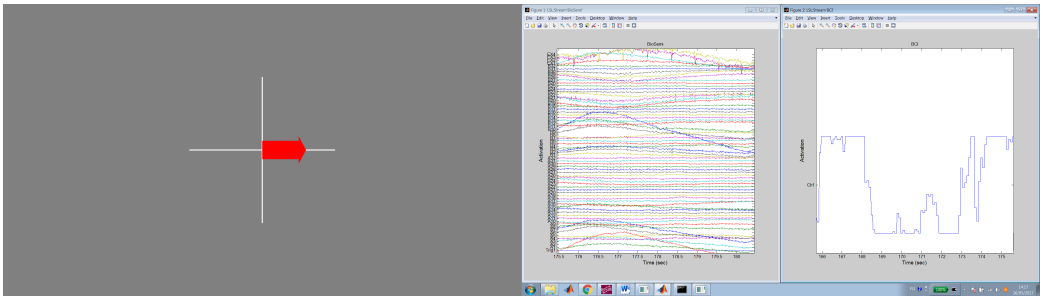

Figure 3.13: Trained models are tested in new training session. In that case, an additional window showing the BCI prediction is displayed on the experimenter's screen. High levels correspond to a high probabilities of right hand imagination.

Once this second training session is finished, $BCI\_2b\_online\_accuracy.m$ computes the accuracy of the current classifier by comparing for each time point the prediction of the model with the target classes indicated by the cued paradigm. If the accuracy is not satisfying, a new model is trained based on the recordings of all training sessions performed so far and is then applied in a third session. When a sufficiently accurate model is obtained, the robotic hand is enabled and the subject is given the possibility to try to control it. This is done using $BCI\_3\_feedback\_session.m$. This session is not recorded and really aims at allowing the subject to get familiar with the time response of the BCI and feel the limits of the system. If the subject does not report feeling in control of the robotic hand, additional training sessions are performed. When the subject feels sufficiently in control of the artificial hand, the training is finished and the task $BCI\_4\_IB.m$ is performed.

The subject is wearing the BioSemi headset during the whole experiment. The signal coming from the electrodes is sent to the Lab Streaming Layer (LSL). As explained in section 2.3.2, LSL is a low level technology that allows synchronized exchanges of time series data between programs and computers. Several streams have to be exchanged between the hardware and the software. This exchange is mainly performed through LSL using a matlab library $liblsl$ or with external executable files, except for the robotic hand for which the communication is done through a serial communication (see figure 3.14). The BCI reads the incoming EEG signal from the Lab Streaming Layer, processes it according to the approach described in section 3.2.3, and writes its predictions on a serial port to control the robotic hand, and to the Lab Streaming Layer for visualization and recording.

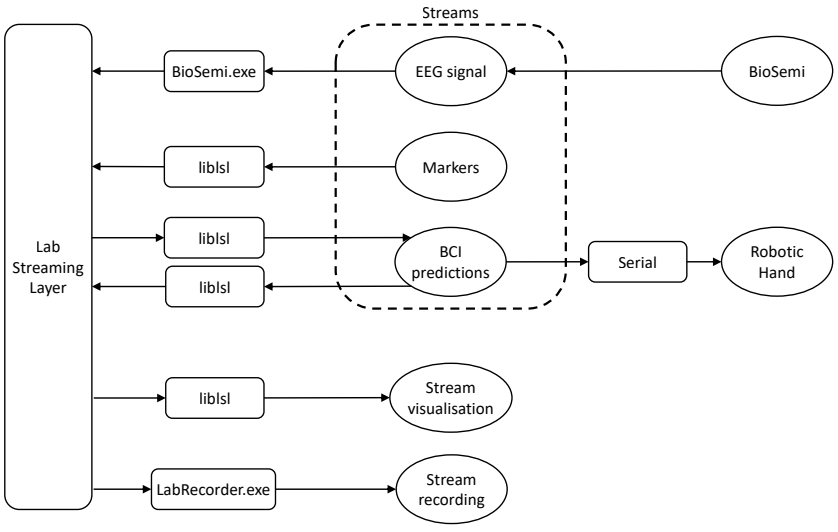

Figure 3.14: The different pieces of hardware and software are communicating with each other through the Lab Streaming Layer described in section 2.3.2

This chapter detailed the implementation of the Brain Computer Interface. First, section 3.1 restated the requirements in terms of technical requirements. Secondly, section 3.2.1 detailed 3 preselected methods. These methods were tested on the data set IIb from the BCI competition IV in section 3.2.2. The implemented BCI would have ranked 6th among the competitors (see section 3.2.3). Finally, section 3.3 described the experimental setup that was designed, as well as the architecture of the implemented algorithm.

Chapter 4

Validation

The Brain Computer Interface described in chapter 3 was designed based on publicly available data. Real tests on voluntary subjects were then needed in order to validate or adapt the algorithm (see section 4.1) before starting the neuroscientific experiment described in section 4.2.

4.1 Calibration and pre-test

These pre-tests also allowed to receive a feedback from the subjects under test and from the neuroscientific researcher in charge of the final experiment. Here are the modifications made to the BCI:

- **Acquisition**:
  In section 3.2.2, the number of electrodes was limited. Using the BioSemi ActiveTwo with 64 electrodes, the number of electrodes becomes an important parameter to tune. As explained in 3.2.1, only the electrodes around the motor cortex were selected in order to minimize the influence of eye artifacts. The 15 selected eletrodes are shown in figure 4.1. Additionnaly, two electrodes were placed at the mastoids to rereference the signal.

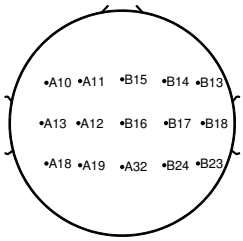

Figure 4.1: The 15 chosen electrodes are indicated using the BioSemi nomenclature (see appendix A for the correspondence with the classical 10-20 system).

- **Cued paradigm**:
  During the cued paradigm, the cross was at first removed in between each trial, right after the imagery period. However, some subjects reported being disturbed when the cross appeared. For one subject, this problem even reflected in the signal, for which the changes in the μ rhythm directly started when the cross appeared. Consequently, it was decided to keep the cross displayed during the whole run. Other modifications concerning the cued paradigm concern the duration of the different periods. These were reduced in order to decrease the length of the training sessions, and the computation time. Indeed, as the algorithm searches for the best time window within the period of imagery, decreasing the latter reduces the amount of windows computed, hence the computational cost. In conclusion, the cued paradigm now starts with $3s$ with a blank cross displayed on a grey screen. After these 3 seconds, a red arrow pointing to the right is superimposed on the cross during $3s$. After that, the arrow is removed but the cross is kept during $2s$. The markers used for classification are added at the beginning of the 3 first seconds of cross display, and when the arrow appears on the screen. This is shown in figure 4.2. Each training session is composed of 20 trials and lasts then $160s$.

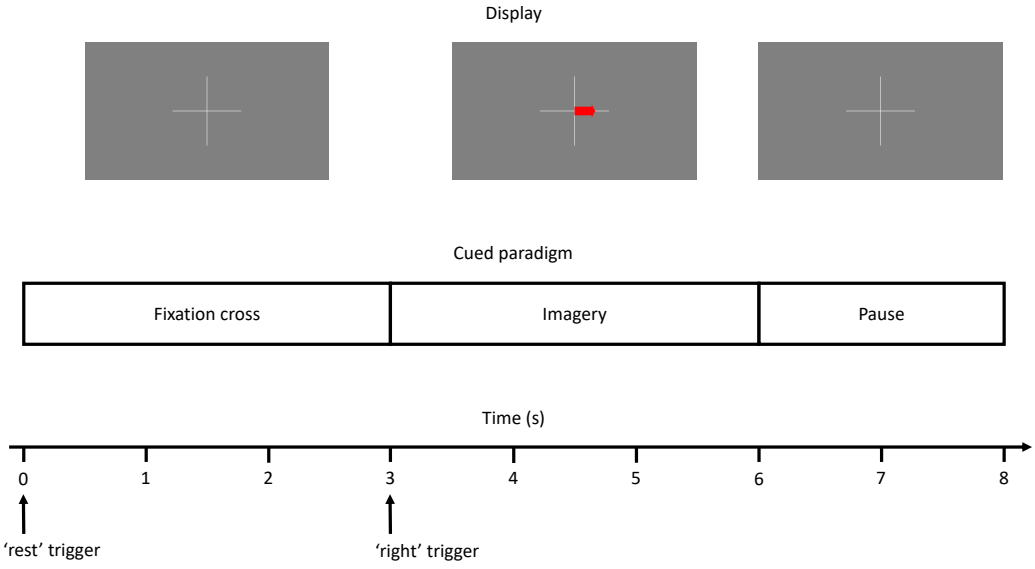

Figure 4.2: In the final cued paradigm, it was decided to keep the fixation cross displayed during the pause to avoid disturbing the participants with too much visual changes on the screen.

- **Feedback**:
  The script $BCI\_1\_training\_session.m$ actually allows to superimposed

a feeback bar on the display, similarly to what is done in many studies (see section 2.2.5). However, participants reported to be distracted by this moving bar. Consequently, it was decided to remove it from the display and have an separated feedback session where the participants are free to test their control on the robotic hand without any imposed cue.

- **Robotic Hand**:
  The finger of the robotic hand can be activated individually. However, when activated, they bent during a certain delay an then went back to initial open position. For the final experiment, the robotic hand must press a key the same way one would do with his real hand. Consequently, the delay was tuned in order to have a movement as realistic as possible. For this experiment, the index finger is bent during $100ms$. On the other hand, during the continuous feedback session, the robotic hand has to stay in activated position until the subject goes back to resting state, which required some modification of the script controlling the hand.

  Additionally, an hysteresis was added in order to avoid parasitic movements of the robotic hand during switching between states during the continuous feedback session. This was implemented using tunable thresholds. The command sent to the robotic hand is based on the probability of movement computed by the classifier. This probability varies between 0 and 1. Three thresholds are introduced:

  1. Lower threshold: this is the value under which the probability has to fall in order to switch from activated state to resting state.
  2. Upper threshold: this is the value above which the probability has to climb in order to switch from resting state to activated state
  3. Middle threshold: this threshold is used for the final experiment. Indeed, for this experiment, the robotic hand only needs to be activated a single time to press the key. When this threshold is exceeded, the robotic hand press the key using the chosen delay and is then deactivated until the next trial.

  The values of these thresholds allow to slightly adapt the difficulty of controlling the robotic hand. As most participants found it much easier to activate the hand than to relax, the thresholds were tuned as follows:

  - Lower threshold:0.5
  - Upper threshold: 1
  - Middle threshold: 1

Six participants were tested, among which 5 males and 1 female. Subject 5 was left-handed, while all other participants were right-handed. The results expressed in terms of accuracy (see section 2.2.4) are shown in table 4.1.

	1st model		2nd model		3rd model		4th model	
	offline	online	offline	online	offline	online	offline	online
S1	75%	56.7%	80%	68.1%	87.5%	61%		
S2	62.5%	48.6%	61.2%	56.5%	58.3%	63.8%	61.2%	58.35%
S3	92.5%	69.9%	88.7%	66.8%				
S4	62.5%	63%	67.5%	52.6%	71.7%	58.5%	71.9%	55.2%
S5	80%	70.9%	81.2%	63%				
S6	85%	58.6%	78.7%	66.1%				

Table 4.1: 6 participants performed the iterative training procedure. Subjects S1, S3, S5 and S6 reached a sufficiently high accuracy during the training sessions and were allowed to perform the feedback session. Each of them reported having a certain control on the robotic hand. Results of subjects S2 and S4 were not satisfying, even after 5 sessions.

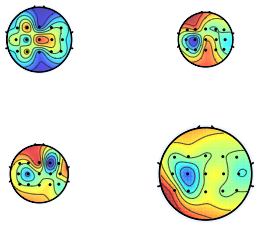

(a) Subject 1: patterns computed for the 2nd model.

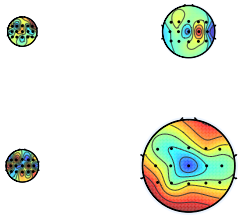

(b) Subject 3: patterns computed for the 1st model.

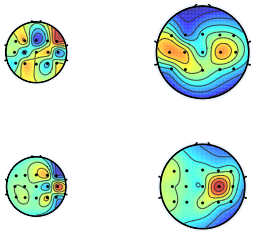

(c) Subject 5: patterns computed for the 1st model.

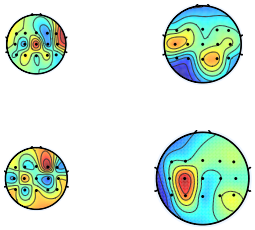

(d) Subject 6: patterns computed for the 2nd model.

Figure 4.3: For each subject, the first row shows the pair of patterns computed for the first frequency band: $8-12Hz$. The second row shows the patterns in the bands $13-30Hz$. The nose is pointing upwards. The patterns are weighted according to their importance in the discrimination task.

The spatial patterns computed by FBCSP for participants S1, S3, S5 and S6

are shown in figure 4.3. Subjects s1 and subject s6 showed expected patterns enhancing the left motor area of the brain, at electrode C3. Patterns of subject S3 enhance the central electrode Cz. Unexpectedly, patterns of subject s5 enhance the right motor area at electrode C4. Whether this is linked to the fact that participant s5 was left-handed remains to be studied. The fact that different patterns are computed according to the subject is one of the strength of the Common Spatial Pattern method.

Models computed for subjects S1, S2, S3 and S5 converged in the iterative training process and were very similar from one session to another. On the contrary, patterns of subjects S2 and S4 constantly changed at each session, meaning that the algorithm did not find any consistent feature to enhance. Consequently, Subject S2 and S4 performed up to 5 training sessions, resulting in 4 different models, but did not reach a satisfying accuracy. Subject S2 still performed the feedback session but did not report feeling in control of the robotic hand. Subject S4 did not performed the feedback session. The fact that these participants did not succeed in controlling the robotic hand could be explained by the fact that they were changing their strategies at each session, or that they were using strategies that involve other frequency bands or other brain areas than the one expected. In the latter case, using more electrodes and more frequency bands could solve the problem but would increase the risk of contamination by artifacts.

These pre-tests showed results similar to those obtained with the data set from the BCI competition. The level of control achieved for 4 out of the 6 participants was judged satisfying. Moreover, the training time was below the 30min specified in the requirements. Given these results, the BCI was validated and the neuroscientific experiment was planned.

4.2 Neuroscientific experiment

This section describes the neuroscientific experiment that was mentioned throughout the previous chapters. It was written in collaboration with Dr. Caspar from the Consciousness, Cognition & Computation Group. First, the context, the implications and the objectives of this study are recalled and detailed. Second, the methodology is described. Finally, the obtained results are discussed.

The study of the control of a robotic hand through a Brain Computer Interface has several major implications in psychology. First, it might help to understand better the factors that increase the feeling of control over the robotic hand, which may be useful in order to increase the perception of autonomy of patients receiving a neuroprosthesis. Second, it might help to understand whether or not sensorimotor information that we receive for instance in our fingers when

we perform an action is a necessary condition for experiencing a sense of control over our voluntary actions. A BCI coupled with a robotic hand indeed allows to perform intentional movements with the robotic hand without receiving the sensorimotor information associated with the action. This will give important results considering the ahead growth of neuroprostheses coupled with sensorimotor captors and on their importance to increase the degree of control, and thus, the autonomy of patients.

In psychology, the experience of being in control of our actions refers to the feeling of agency, that is, the feeling that you are the author of your own actions and their consequences (Gallagher, 2000). There are two main methods to assess the sense of agency. The first one is based on explicit questions asked to participants after an action (e.g. 'Were you the author of that action?') and refers to what is called explicit judgments of agency. However, these measurements are known to be biased by different factors, such as social desirability (Bandura, 2006) and thus appear to be less reliable. Another method based on a methodological innovation proposes to use time perception as an implicit marker of agency, a method called the 'intentional binding' (Haggard, Clark, & Kalogeras, 2002) . In a classical intentional binding paradigm, participants have to estimate the delay between their action (i.e. a keypress) and an outcome (i.e. a tone). If the movement is voluntary, the perceived time is shorter than in a condition in which the movement is involuntary (for instance, triggered by a Transcranial Magnetic Stimulation (TMS) pulse over the motor cortex), suggesting that sense of being the author of an action modifies time perception, by reducing it. This method has been validated in an important amount of scientific papers so far (see (Moore, 2016) for a review) and is now used to infer about the agentic state of participants in a given task. In addition, the sense of agency has been intimately linked to the phenomenon of sensory attenuation. Sensory attenuation refers to the observation that self-generated stimuli appear to be attenuated in terms of their cortical response compared to the same stimuli when they are generated by an external source, for instance, by someone else. Consequently, it has been assumed that sensory attenuation might help individuals to determine whether a sensory event was caused by themselves or not, which also provide important information about their perception of being the author of that action (i.e. sense of agency).

In this context, the Consciousness, Cognition & Computation Group wanted to realise a pilot experiment in order to determine: 1) the ratio of participants who are able to successfully control the robotic hand through a BCI after a few training sessions, 2) whether or not the cognitive fatigue associated with controlling a BCI would interfere with their implicit measure of the sense of agency (i.e. the method based on time perception) and 3) whether some correlations between the degree of control that participants feel about the BCI would influence the

implicit measures of agency and the sensory attenuation process, as measured by the amplitude of the auditory N1, an evoked potential associated with the tone. These preliminary results would give them important elements in order to consider the final experiment.

Method Twenty-three participants were invited to participate in the present study. All participants provided written informed consent prior to the experiment. The study was approved by the local ethical committee of the Université libre de Bruxelles (054/2015).

Participants were equipped with an electroencephalogram at the beginning of the experiment. Then, they performed an intentional binding paradigm without the robotic hand. In this task, the participant was instructed to press a key on the keyboard at a time he chose after the start of the trial. A tone occurred after the key press. The delay between the key press and tone varied randomly at 100, 500, and $900ms$. The participants' task was to estimate the delay between the key press and the tone (=intentional binding procedure). They were informed that the delay would vary randomly on a trial-by-trial basis, between 1 and $1,000ms$ (they were reminded that $1,000ms$ equals $1s$). Participants were also told: 1) to make use of all possible numbers between 1 and $1,000$, as appropriate, 2) to avoid restricting their answer space (i.e., not to keep using numbers falling between 100 and 200), and 3) to avoid rounding. They had to write down their answer with their left hand. They performed this task during 60 trials.

After this task, participants started the learning sessions as described in section 3.3. Participants were told that they should perform the training session minimum twice and maximum 6 times. The value of accuracy used as threshold was lowered to 55% in order to have variability in the results, with participants having a low degree of control and participants having a high degree of control.

If the model was sufficiently accurate after the training, participants performed once again the intentional binding paradigm but this time with the robotic hand pressing on the key to produce the tone instead of their real hand. Participants were invited to keep their right hand relaxed on their legs and to use their left hand to provide their answers. Two electrodes were placed at the muscular junction controlling the finger movements on their right arm in order to control their muscular activity, to ensure that they did not trigger the movement of the robotic hand by actually producing a real movement with their own right hand. After that participants had provided their numerical answer to estimate the action-tone delay, they were invited to answer, on a scale from 0 to 10, how much they felt that the movement of the robotic hand was caused by their own will. This question aimed at removing false positives.

Brain activity was recorded using a 64-channels electrode cap with the Ac-

tiveTwo system (BioSemi) and data were analysed using Fieldtrip (Oostenveld et al., 2011). The activities from left and right mastoids were also recorded. Amplified voltages were sample at $512Hz$. Data were referenced to the average signal of the mastoids and filtered (low-pass at $50Hz$ and high-pass at $0.01Hz$).

Results On 23 participants, 17 were able to control the BCI (mean accuracy= 63.22%, SD=5.5). Those participants reported in average that they controlled the robotic hand with a precision of 70.80% (SD=16). We performed a Pearson correlation and observed that the theoretical level of accuracy was positively correlated with participants' own perception of control over the robotic hand (r=.490, p=.046). This indicates that the accuracy provided by the model was a good predictor of the participants' perception of controlling the hand.

In order to check whether or not the cognitive fatigue associated with the use of the robotic hand would affect the intentional paradigm, we identified participants whom the action-tone intervals did not gradually increase with action-tone intervals, we performed linear trend analysis with contrast coefficients -1, 0, 1 for the three delays. We performed the same analysis on the action-tone intervals provided in the first intentional binding paradigm (i.e., without the robotic hand). If their answers did progress with the real action-tone intervals in the first intentional binding task (without the robotic hand) but not in the second intentional binding task (with the robotic hand), it would suggest that BCI involves a too important cognitive fatigue. On the 17 participants, 2 showed a non-significant trend in the second intentional binding task while their trend was significant in the first intentional binding task. It thus suggests that we can expect to keep 65% of our sample with the current version of the BCI.

Additional correlations were performed between the reported degree of control of participants, the amplitude of the auditory N1 and the intentional binding. None of those correlations were significant (all ps $>$ .3). However, the sample of participants was not sufficiently high to expect reliable significant results. For correlational analyses, the requested sample is generally about 30.

In this chapter, the implemented BCI was tested first on a small sample of 6 participants (see section 4.1). This pre-test allowed to calibrate and adapt the algorithm implemented in chapter 3. The obtained results being satisfying, a pivot experiment was conducted on a sample of 23 participants (see section 4.2). This pivot experiment allowed to test 2 hypothesis and showed promising results for future experiments.

Chapter 5

Discussion

This chapter discusses the results obtained in chapter 3 and 4.

The Brain Computer Interface implemented in the present work was designed based on the publicly available data set IIb from the BCI competition IV. As detailed in section 3.2.3, it would have ranked 6th among the competitors. Considering that these competitors were research groups composed of 2 to 6 researchers (Tangermann et al., 2012), the results obtained in the present master thesis are very satisfying. However, one should not forget that the true labels for the test data sets were only made available at the end of the competition. Hence, initial competitors could not use them to tune their algorithms. Moreover, the Matlab toolbox used in this work was developed after this competition and was clearly influenced by it. Indeed, most of the methods used by the competitors were added to the toolbox, including Filter Bank Common Spatial Pattern.

Compared to the winning algorithm described in (Ang et al., 2012), the present BCI has a time response 2 times faster. Indeed, they used a window of $2s$ for the feature extraction, meaning that the ouput of the BCI is delayed of $2s$ too. In the present work, this window length was limited to $1s$ to meet the requirements. The further decreasing of this parameter is limited by the physical time constant involved in the underlying neural mechanism. The μ band ranging from 8 to $12Hz$, one period lasts around $10ms$. In order to properly measure the decrease of amplitude due to the Event-Related Desynchronization (see 2.2.2), the time window should contain more than one single period. Decreasing the length of the time window means decreasing the number of periods used for the computation. Consequently, either the algorithm must be improved to be able to deal with this limited amount of data, or the user has to learn producing better signals. The latter solution could be achieved by using most advance learning and feedback methods (see 2.2.5).

The accuracy obtained on this data set stays below the 75% specified in the technical requirements. Looking at the individual performance of the subjects, 2 participants out of 9 reached results above the 75% threshold for the left versus right hand movement condition. This corresponds to 22.22% of participants for which the BCI worked, which is below the 50% specified in the requirements. When considering the rest versus right hand movement condition, no subject exceeded the 75% threshold. However, as explained in section 3.2.3, the experiment was not initially designed for this second condition.

Those results needed to be confirmed on an adapted experimental setup. This was done in section 4.1. 6 participants were tested. The accuracy obtained was slightly better: $66.83 \pm 3.03\%$ against $64.67 \pm 5.98\%$. No participant did exceed the 75% threshold. However, 4 out of the 6 participants reported having control on the robotic hand. This was the main objective and regarding this the BCI successfully achieved its task for 66.66% of the participants during these pre-tests. This percentage is well above the 50% expressed in the requirements. Regarding these results, the accuracy value used as threshold was reconsidered. Indeed, the work from which it was taken, studied a left versus right hand movement condition (Evans et al., 2015). The resting condition being more challenging (Tangermann et al., 2012), a lower accuracy is expected. Moreover, it is important to remember that the data set IIb from the BCI competition contains much more trials than the paradigm implemented in the present study. The participant followed 5 sessions containing each 60 trials of each class (see section 3.2.2). In comparison, the implemented paradigm contains 20 trials of each class for each session. The accuracy obtained is then of the same order of magnitude with a classifier trained on 3 times less data. This reduction of the number of trials was needed to meet the requirements about the allowable training time. With the current implemented cued paradigm, each training session lasts $2min40$ (see section 4.1). Taking into account the time needed to launch the script, for the participant to get ready, and for the computation of the model, the total duration of a training session is about $5min$. $30min$ are then enough to do 5 to 6 sessions.

The BCI being validated through these pre-tests, a pilot experiment was conducted by Dr. Caspar from the Consciousness, Cognition & Computation Group (see 4.2). This experiment allowed to validate several aspects of the implemented BCI. First of all, 65% of the sample was kept, which confirmed the results obtained during the pre-tests. Secondly, the training time stayed below 30*min*. Concerning this point, it was also shown in 4.2 that the training sessions were not cognitively too demanding. Hence, the BCI training procedure is compatible with an additional cognitive task (i.e. intentional parardigm), which is essential

for the present work. Thirdly, the average accuracy of 63.22% was similar to the one obtained during the pre-tests. This result, as already said, is very satisfying given the limited training time. Finally, the interface was used without any problem by the experimenter.

As conclusion, the implemented BCI has already proven that it is fully operational. The pivot experiment already allowed to test 2 hypothesis that will be helpful for the future experiments. Theses results are very promising and open new possibilities in the research about the sense of agency.

Limitations The implemented BCI was validated for a 2 classes problem. Even if the BCILAB toolbox does not restrict the number of classes, a complete validation is needed to test the feasibility of such a BCI.

The resting class still remains a challenge. Indeed, most participants reported having more difficulties with this class than the other class. They had to concentrate about something else rather than really being resting.

The accuracy computed during the training session barely exceeds 70%. One participant reached an impressive accuracy of 77.3%. Solution should be found to improve this accuracy in case of more advanced experiments involving more complex tasks.

Future work In the context of neuroscientific research, future work could evaluate more advanced training methods involving more adapted learning mechanisms. This would be a very interesting topic to try to improve the accuracy of the classifier without increasing the training time. Outside of the neuroscientific research, there would be a need for increasing the number of classes. 4 classes motor imagery BCI's have been realized (see data set IIa from BCI competition IV (Tangermann et al., 2012)) but mostly involved very different tasks such as left hand movement, right hand movement, foot movement and tongue movement. Being able to discriminate different movements of one single hand would be a tremendous step ahead. This would require improvements in the acquisition device. Also related to the acquisition, dry electrodes are a must for the use of BCI's outside lab environment.

Chapter 6

Conclusion

The goal of this work was to implement a Brain Computer Interface to help neuroscientists develop new experiments to explore mechanisms related to the sense of agency.

As an extension of the previous study about the sense of agency involved when controlling a robotic hand (Caspar et al., 2014), the neuroscientific experiment required the subject to be able to activate a robotic hand at will, directly through his mind.

After a review of the State of the Art, it was decided to implement the BCI on Matlab using the BCILAB toolbox. The BCI takes as input the EEG activity recorded using a BioSemi ActiveTwo. Then, Filter Bank Common Spatial Pattern and Linear Discriminant Analysis are used to discriminate an imagined movement from a resting state. If a movement is predicted, a command is sent to a robotic hand that was designed specifically for this kind of experiment (De Beir et al., 2014).

The BCI was implemented and tested first on publicly available data sets from the BCI competition IV. Secondly, it was tested on a small sample of 6 participants. Finally, a pilot experiment was conducted on a sample of 23 participants, giving very promising results for future experiments.

Appendix A

BioSemi

Sample-rate options (sample rate is adjustable by user)	2048 Hz	4096 Hz	8192 Hz	16,384 Hz
Max. number of channels @ selected sample rate	280	280	280	152
Bandwidth (-3dB)	DC - 400 Hz	DC - 800 Hz	DC - 1600 Hz	DC - 3200 Hz
Low-pass response	5th order sinc digital filter			
High-pass respons	fully DC coupled			
Digitalization	24 bit, 4th order Delta-Sigma modulator with 64x oversampling, one converter per channel			
Sampling skew	<10 ps			
Absolute sample rate accuracy (over temp range 0-70 C)	0.1 Hz	0.2 Hz	0.4 Hz	0.8 Hz
Relative sample rate accuracy (jitter)	<200 ps			
Quantization-resolution	LSB = 31.25 nV, guaranteed no missing codes			
Gain accuracy	0,3 %			
Anti aliasing filter	fixed first order analog filter, -3dB at 3.6 kHz			
Total input noise (Ze <10 kOhm), full bandwidth	0.8 uVRMS (5 uVpk-pk)	1.0 uVRMS (6 uVpk-pk)	1.4 uVRMS (8 uVpk-pk)	2.0 uVRMS (12 uVpk-pk)
1/f noise (Ze <1 MOhm)	1 uVpk-pk @ 0.1..10Hz			
Amplifier current noise	<30 fArms			
Input bias current	<100 pA per channel			
Input impedance Active Electrode	300 MOhm @ 50 Hz (1012 Ohm // 11 pF)			
DC offset	<0.5 mV			
DC drift	<0.5 uV per degree Celsius			
Input range	+262 mV to -262 mV			
Distortion	<0.1 %			
Channel separation	>100 dB			
Common Mode Rejection Ratio	>90 dB @ 50 Hz			
Isolation Mode Rejection Ratio	>160 dB @ 50 Hz			
Power Consumption	4 Watt @ 280channels inversely proportional with the number of installed channels			
Battery capacity, standard battery	25 Watt-hour, 3 cell sealed lead-acid (double capacity battery is available as an option)			
Battery life on standard battery	>5 hours @ 280channels inversely proportional with the number of installed channels			
Battery charge time (with external fast charger)	<3.5 hours for a 100% charge			
Leakage current, normal operation	<1 uA rms.			
Leakage current, single fault	<50 uArms			
Trigger inputs	16 inputs on optical receiver (isolated from subject section) , TTL level			
Trigger outputs	15 outputs on optical receiver (isolated from subject section) , TTL level			
PC interface	USB2.0			
Size of front-end, including battery-box (H x W x D)	120 x 150 x 190 mm			
Weight of front-end, including battery-box	1.1 kg			
Warranty	3 years			

Table A.1: Detailed specifications of the BioSemi ActiveTwo

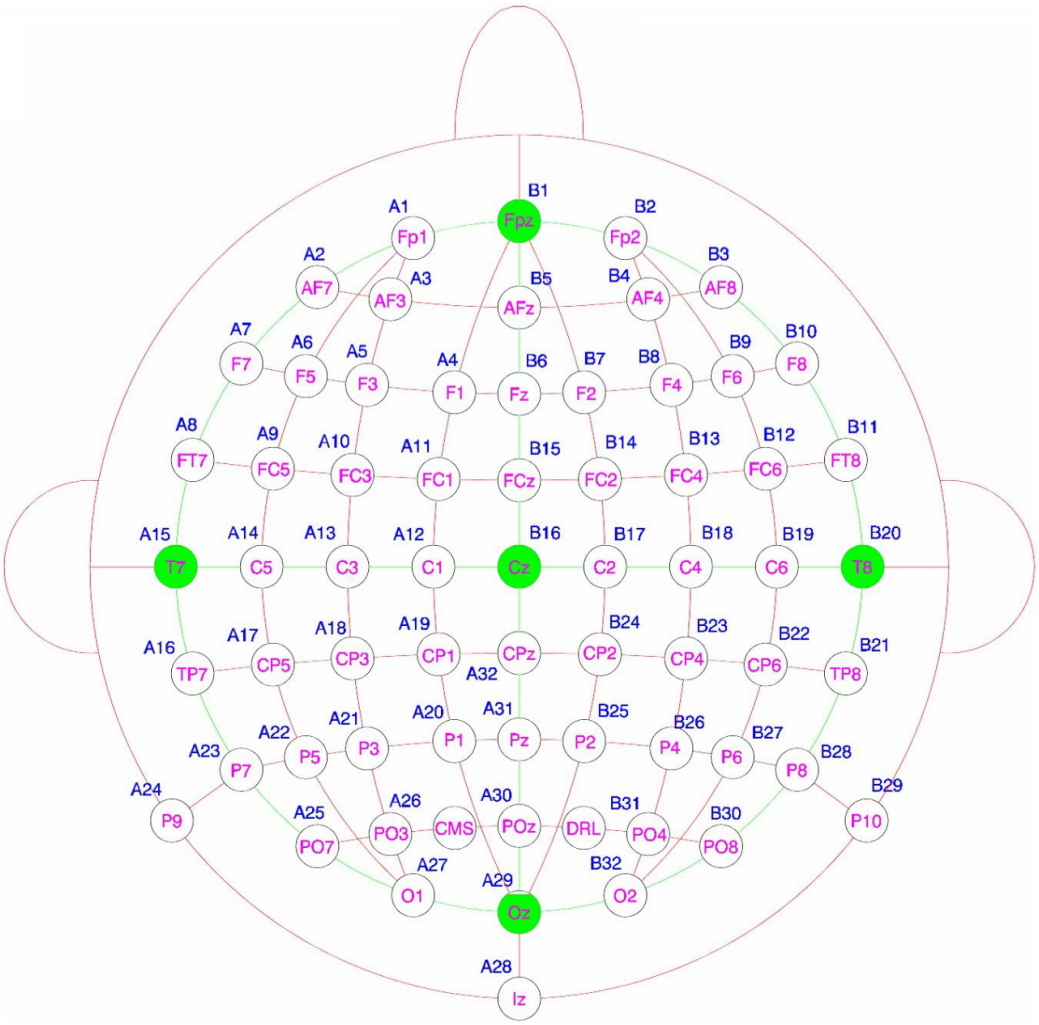

Figure A.1: Electrode placement of the BioSemi ActiveTwo

Appendix B

Results of the pilot experiment

IDt	Age	Gender	Model used	Accuracy	IB 100	IB 500	IB 900	Mean reported control	IB BCI 100	IB BCI 500	IB BCI 900	IB Real Hand	IB Robot Hand	N1 TOTAL
1	21	F	2	62,63	13,1	24,15	47,2	72,93	40,66	47,55	48,88	28,15	45,70	
3	22	M	3	64	385	569,5	709,95	52,33	390,05	539,57	487,78	554,82	472,47	-8,949
5	19	F	4	65,65	52,25	118,2	374,05	71,66	421	325,57	491,15	181,50	412,57	-3,76
6	20	F	1	63,4	294,52	486,66	812,8	53,89	365,57	615,75	857,27	531,33	612,86	
7	25	F	5	63,65	186,89	461,35	766,42	55,83	196,23	275,94	502,85	471,55	325,01	-11,89
8	20	F	3	68,71	181,21	378,89	697,31	85	307,68	461,25	679,1	419,14	482,68	
9	20	F	3	61,7	323,47	632,15	908,36	64,4	559,15	759,63	704,15	621,33	674,31	1,011
10	24	M	4	59,4	294,35	342,27	624,05	51,16	555,1	616,45	759,57	420,22	643,71	-11,7
11	21	F	3	63,6	390,73	492,68	787,1	51,66	428,21	569,94	705,95	556,84	568,03	-4,358
12	19	F	2	63,6	310,52	303,72	570,3	93	389,9	602,3	679,15	394,85	557,12	-7,846
14	18	F	5	59,4	126,52	312	498,75	80,66	200,61	229,78	316,7	312,42	249,03	-1,396
15	22	F	1	59,8	226,55	663,84	797,47	59,33	304,84	382	582,95	562,62	423,26	
16	19	F	2	70,5	366,6	520	769,45	99,66	506,45	618,84	701,52	552,02	608,94	
18	18	F	3	77,3	304,65	392	437,73	92,33	548,31	705,05	603,89	378,13	619,08	-7,04
19	18	M	1	62,2	261,9	442,89	586,9	81,5	410	448,89	479,57	430,56	446,15	-2,129
20	24	M	2	55,8	201,05	522,4	881,94	76,5	337,21	648	908,89	535,13	631,37	-6,737
22	22	M	4	53,4	280,05	486,75	839,44	61,83	632,05	763,94	850,3	535,41	748,76	-3,896

Table B.1: Results of the pilot experiment

References

Al-ani, T., & Trad, D. (2010). *Signal processing and classification approaches for brain-computer interface*. INTECH Open Access Publisher.

Alimardani, M., Nishio, S., & Ishiguro, H. (2016). Removal of proprioception by bci raises a stronger body ownership illusion in control of a humanlike robot. *Scientific Reports*, *6*.

Ang, K. K., Chin, Z. Y., Wang, C., Guan, C., & Zhang, H. (2012). Filter bank common spatial pattern algorithm on bci competition iv datasets 2a and 2b. *Frontiers in Neuroscience*, *6*.

Ang, K. K., Chin, Z. Y., Zhang, H., & Guan, C. (2008). Filter bank common spatial pattern (fbcsp) in brain-computer interface. In *Neural networks, 2008. ijcnn 2008.(ieee world congress on computational intelligence). ieee international joint conference on* (pp. 2390–2397).

Bandura, A. (2006). Toward a psychology of human agency. *Perspectives on psychological science*, *1*(2), 164–180.

Berger, H. (1929). Über das elektrenkephalogramm des menschen. *European Archives of Psychiatry and Clinical Neuroscience*, *87*(1), 527–570.

Blankertz, B., Blankertz, B., Tomioka, R., Tomioka, R., Lemm, S., Lemm, S., ... Müller, K.-R. (2008). Optimizing Spatial Filters for Robust EEG Single-Trial Analysis. *Ieee Signal Processing Magazine*, *XX*, 1–12. doi: 10.1109/MSP.2008.4408441

Blankertz, B., Lemm, S., Treder, M., Haufe, S., & Müller, K.-R. (2011). Single-trial analysis and classification of erp componentsâa tutorial. *NeuroImage*, *56*(2), 814–825.

Blankertz, B., Müller, K.-R., Krusienski, D. J., Schalk, G., Wolpaw, J. R., Schlögl, A., ... Birbaumer, N. (2006). The bci competition iii: Validating alternative approaches to actual bci problems. *Neural Systems and Rehabilitation Engineering, IEEE Transactions on*, *14*(2), 153–159.

Botvinick, M., Cohen, J., et al. (1998). Rubber hands' feel'touch that eyes see. *Nature*, *391*(6669), 756–756.

Braun, N., Emkes, R., Thorne, J. D., & Debener, S. (2016). Embodied neurofeedback with an anthropomorphic robotic hand. *Scientific Reports*, *6*.

Buzsaki, G. (2006). *Rhythms of the brain*. Oxford University Press.

Caspar, E. A., Christensen, J. F., Cleeremans, A., & Haggard, P. (2016). Coercion changes the sense of agency in the human brain. *Current biology*, *26*(5), 585–592.

Caspar, E. A., Cleeremans, A., & Haggard, P. (2015). The relationship between human agency and embodiment. *Consciousness and cognition*, *33*, 226–236.

Caspar, E. A., De Beir, A., Da, P. A. M. D. S., Yernaux, F., Cleeremans, A., Vanderborght, B., et al. (2014). New frontiers in the rubber hand experiment: when a robotic hand becomes one's own. *Behavior research methods*, 1–12.

Cincotti, F., Bianchi, L., Birch, G., Guger, C., Mellinger, J., Scherer, R., ... Schalk, G. (2006). Bci meeting 2005-workshop on technology: hardware and software. *IEEE Transactions on Neural Systems and Rehabilitation Engineering*, *14*(2), 128–131.

De Beir, A., Caspar, E., Yernaux, F., Da Saldanha da Gama, P. M., Vanderborght, B., & Cleermans, A. (2014). Developing new frontiers in the rubber hand illusion: Design of an open source robotic hand to better understand prosthetics. In *Robot and human interactive communication, 2014 ro-man: The 23rd ieee international symposium on* (pp. 905–910).

Delorme, A., & Makeig, S. (2004). Eeglab: an open source toolbox for analysis of single-trial eeg dynamics including independent component analysis. *Journal of neuroscience methods*, *134*(1), 9–21.

Durka, P., Kuś, R., Żygierewicz, J., Michalska, M., Milanowski, P., Łabęcki, M., ... Kruszyński, M. (2012). User-centered design of brain-computer interfaces: Openbci. pl and bci appliance. *Bulletin of the Polish Academy of Sciences: Technical Sciences*, *60*(3), 427–431.

Evans, N., Gale, S., Schurger, A., & Blanke, O. (2015). Visual Feedback Dominates the Sense of Agency for Brain-Machine Actions. *PloS one*, *10*(6), e0130019. Retrieved from http://journals.plos.org/plosone/article?id=10.1371/journal.pone.0130019 doi: 10.1371/journal.pone.0130019

Fatourechi, M., Bashashati, A., Ward, R. K., & Birch, G. E. (2007). Emg and eog artifacts in brain computer interface systems: A survey. *Clinical neurophysiology*, *118*(3), 480–494.

Gallagher, S. (2000). Philosophical conceptions of the self: implications for cognitive science. *Trends in cognitive sciences*, *4*(1), 14–21.

Grozea, C., Voinescu, C. D., & Fazli, S. (2011). Bristle-sensorsâlow-cost flexible passive dry eeg electrodes for neurofeedback and bci applications. *Journal of neural engineering*, *8*(2), 025008.

Hagemann, D., Naumann, E., & Thayer, J. F. (2001). The quest for the eeg

reference revisited: a glance from brain asymmetry research. *Psychophysiology*, *38*(5), 847–857.

Haggard, P., Clark, S., & Kalogeras, J. (2002). Voluntary action and conscious awareness. *Nature neuroscience*, *5*(4), 382.

Hjorth, B. (1975). An on-line transformation of eeg scalp potentials into orthogonal source derivations. *Electroencephalography and clinical neurophysiology*, *39*(5), 526–530.

Kothe, C. A., & Makeig, S. (2013). Bcilab: a platform for brain–computer interface development. *Journal of neural engineering*, *10*(5), 056014.

Leeb, R., Brunner, C., Müller-Putz, G., Schlögl, A., & Pfurtscheller, G. (2008). Bci competition 2008–graz data set b. *Graz University of Technology, Austria*.

Lopez-Gordo, M., Sanchez-Morillo, D., & Valle, F. P. (2014). Dry eeg electrodes. *Sensors*, *14*(7), 12847–12870.

Lotte, F. (2012). On the need for alternative feedback training approaches for bci. In *Berlin brain-computer interface workshop.*

Lotte, F., Congedo, M., Lécuyer, A., & Lamarche, F. (2007). A review of classification algorithms for eeg-based brain–computer interfaces. *Journal of neural engineering*, *4*.

Lotte, F., & Jeunet, C. (2015). Towards improved bci based on human learning principles. In *Brain-computer interface (bci), 2015 3rd international winter conference on* (pp. 1–4).

Moore, J. W. (2016). What is the sense of agency and why does it matter? *Frontiers in Psychology*, *7*.

Müller-Gerking, J., Pfurtscheller, G., & Flyvbjerg, H. (1999). Designing optimal spatial filters for single-trial eeg classification in a movement task. *Clinical neurophysiology*, *110*(5), 787–798.

Nijboer, F., van de Laar, B., Gerritsen, S., Nijholt, A., & Poel, M. (2015). Usability of three electroencephalogram headsets for brain–computer interfaces: a within subject comparison. *Interacting with computers*, iwv023.

Oostenveld, R., Fries, P., Maris, E., & Schoffelen, J.-M. (2011). Fieldtrip: open source software for advanced analysis of meg, eeg, and invasive electrophysiological data. *Computational intelligence and neuroscience*, *2011*, 1.

Pfurtscheller, G., & Da Silva, F. L. (1999). Event-related eeg/meg synchronization and desynchronization: basic principles. *Clinical neurophysiology*, *110*(11), 1842–1857.

Pineda, J. A., Allison, B., & Vankov, A. (2000). The effects of self-movement, observation, and imagination on/spl mu/rhythms and readiness potentials (rp's): toward a brain-computer interface (bci). *IEEE Transactions on Rehabilitation Engineering*, *8*(2), 219–222.

Renard, Y., Lotte, F., Gibert, G., Congedo, M., Maby, E., Delannoy, V., ... Lécuyer, A. (2010). Openvibe: An open-source software platform to design, test, and use brain–computer interfaces in real and virtual environments. *Presence: teleoperators and virtual environments*, *19*(1), 35–53.

Schlögl, A., & Brunner, C. (2008). Biosig: a free and open source software library for bci research. *Computer*, *41*(10).

Schlogl, A., Kronegg, J., Huggins, J., & Mason, S. (2007). 19 evaluation criteria for bci research. *Toward brain-computer interfacing*.

Shimada, S., Fukuda, K., & Hiraki, K. (2009). Rubber hand illusion under delayed visual feedback. *PloS one*, *4*(7), e6185.

Subha, D. P., Joseph, P. K., Acharya, R., & Lim, C. M. (2010). Eeg signal analysis: a survey. *Journal of medical systems*, *34*(2), 195–212.

Suryotrisongko, H., & Samopa, F. (2015). Evaluating openbci spiderclaw v1 headwear's electrodes placements for brain-computer interface (bci) motor imagery application. *Procedia Computer Science*, *72*, 398–405.

Tangermann, M., Müller, K.-R., Aertsen, A., Birbaumer, N., Braun, C., Brunner, C., ... others (2012). Review of the bci competition iv. *Frontiers in neuroscience*, *6*.

Tomioka, R., Dornhege, G., Nolte, G., Blankertz, B., Aihara, K., & Müller, K.-R. (2006). Spectrally weighted common spatial pattern algorithm for single trial eeg classification. *Dept. Math. Eng., Univ. Tokyo, Tokyo, Japan, Tech. Rep*, *40*.

Tompkins, W. J. (1993). Biomedical digital signal processing. *Editorial Prentice Hall*.

Vaughan, T. M., Heetderks, W., Trejo, L., Rymer, W., Weinrich, M., Moore, M., ... others (2003). *Brain-computer interface technology: a review of the second international meeting*.

Vaughan, T. M., & Wolpaw, J. R. (2011). Special issue containing contributions from the fourth international brain–computer interface meeting. *Journal of neural engineering*, *8*(2), 020201.

Wolpaw, J. R., Birbaumer, N., Heetderks, W. J., McFarland, D. J., Peckham, P. H., Schalk, G., ... others (2000). Brain-computer interface technology: a review of the first international meeting. *IEEE transactions on rehabilitation engineering*, *8*(2), 164–173.